Neuropharmacology 58 (2010) 987–1001

Contents lists available at ScienceDirect

Neuropharmacology

journal homepage: www.elsevier.com/locate/neuropharm

Neuroprotective and neuroproliferative activities of NeuroAid (MLC601, MLC901), a Chinese medicine, *in vitro* and *in vivo*

C. Heurteaux [a,*], C. Gandin [a], M. Borsotto [a], C. Widmann [a], F. Brau [a], M. Lhuillier [b], B. Onteniente [b], M. Lazdunski [a,*]

[a] *Institut de Pharmacologie Moléculaire et Cellulaire, Centre National de la Recherche Scientifique (CNRS), Université de Nice Sophia Antipolis, 660 Route des Lucioles, 06560 Valbonne, France*
[b] *INSERM UMR 861, Université d'Evry, 5 rue Henri Desbrueres, 91030 Evry cedex, France*

ARTICLE INFO

Article history:
Received 4 September 2009
Received in revised form
1 December 2009
Accepted 4 January 2010

Keywords:
NeuroAid
Stroke
Focal ischemia
Excitotoxicity
Neurogenesis
Proliferation

ABSTRACT

Although stroke remains a leading cause of death and adult disability, numerous recent failures in clinical stroke trials have led to some pessimism in the field. Interestingly, NeuroAid (MLC601), a traditional medicine, particularly used in China, South East Asia and Middle East has been reported to have beneficial effects in patients, particularly in post-stroke complications. Here, we demonstrate in a rodent model of focal ischemia that NeuroAid II (MLC901) pre- and post-treatments up to 3 h after stroke improve survival, protect the brain from the ischemic injury and drastically decrease functional deficits. MLC601 and MLC901 also prevent neuronal death in an *in vitro* model of excitotoxicity using primary cultures of cortical neurons exposed to glutamate. In addition, MLC601/MLC901 treatments were shown to induce neurogenesis in rodent and human cells, promote cell proliferation as well as neurite outgrowth and stimulate the development of a dense axonal and dendritic network. MLC601 and MLC901 clearly represent a very interesting strategy for stroke treatment at different stages of the disease.

1. Introduction

Stroke affects numerous people every year. When brain cells die, the function of the body parts they control is impaired or lost, causing paralysis, speech and sensory problems, memory and reasoning deficits, coma, and possibly death. Treatment for stroke is almost reduced to fibrinolysis, a therapy that unfortunately can be only used in a relatively low percentage of patients. Dozens of clinical trials have failed to show efficacy in humans for a variety of neuroprotective drugs (Ginsberg, 2008). In addition, there are no effective, clinically approved methods that promote restoration of CNS function, days, weeks or months after stroke. The need for new therapeutic strategies is high.

A slow but consistent recovery can be observed in the clinical practice over a period of weeks and months. Whereas the recovery in the first few days likely results from edema resolution and/or from reperfusion of the ischemic penumbra, a large part of the recovery afterwards is mainly due to brain which spontaneously recovers by the reorganization of surviving central nervous system elements in the damaged areas (Cramer, 2008). Neurogenesis and angiogenesis are key mechanisms of recovery after stroke (Zhang et al., 2008). The research of therapeutic agents able to stimulate proliferation, migration and differentiation of new neural cells that can replace those lost during a stroke episode is important for future.

Due to the complexity of stroke disease, there is increasing evidence that the search for a "magic drug" which specifically acts on a single target is exceeded and that combination therapies comprising more than one active ingredient can represent a better strategy against stroke. Interestingly, combination therapy has been advocated for >2500 years by prescriptions of formulae in traditional Chinese Medicine (TCM), that consist of several types of medicinal herbs, based on clinical experience. As recently shown for promyelocytic leukemia, Chinese herbal medicines can represent a new promising area in drug discovery (Wang et al., 2008). The aim of this work is to address the possible beneficial effects of MLC601 and MLC901 against stroke disease. MLC601 (NeuroAid, Moleac Pte. Ltd, Singapore) is a TCM which is used extensively in China to facilitate recovery after stroke (Chen et al., 2009). It combines 9 herbal (including Radix astragali, Radix salviae miltiorrhizae, Radix paeoniae rubra, Rhizoma chuanxiong, Radix angelicae sinensis, Carthamus tinctorius, Prunus persica, Radix polygalae and Rhizoma acori tatarinowii) and 5 animal components (including Hirudo, Eupolyphaga seu steleophaga, Calculus bovisartifactus, Buthus

* Corresponding authors. Tel.: +33 4 93 95 77 84; fax: +33 4 93 95 77 04.
E-mail addresses: heurteau@ipmc.cnrs.fr (C. Heurteaux), lazdunski@ipmc.cnrs.fr (M. Lazdunski).

0028-3908/$ – see front matter © 2010 Elsevier Ltd. All rights reserved.
doi:10.1016/j.neuropharm.2010.01.001

martensii and Cornu saigae tataricae). A simplified formula of MLC601 called MLC901 (NeuroAid II) based on its 9 herbal components is now also available. A multicenter, randomized, double-blind placebo-controlled study to investigate CHInese Medicine MLC601 Efficacy on Stroke recovery (CHIMES) is ongoing in Asia (Venketasubramanian et al., 2009). Additional studies assessing immediate and long-term effects, alone or in combination with aspirin showed the safety of MLC601 in normal subjects and stroke patients (Gan et al., 2008; Siow, 2008). However, before this work was started, there was no scientific background for the use of this TCM against stroke. The purpose of this work is to analyze whether MLC601 and MLC901 have interesting neuroprotective and/or neurogenerative properties in *in vitro* and *in vivo* assays that are normally used in Western medicine to develop new drugs, preclinically, before assaying them in humans. We report here the protective effects of MLC601 and MLC901 on neuronal and brain injuries as well as positive effects on functional recovery after ischemic stroke. We also demonstrate *in vitro* neuronal proliferation and neurite outgrowth as well as *in vivo* neurogenesis induced by MLC601/MLC901.

2. Materials and methods

2.1. Neuronal culture

Time-pregnant (E14) C57Bl/6J mice were anesthetized with isopentane followed by cervical dislocation. Fetuses were removed and placed in cold $HBSS^+$ solution. Cerebral cortices were dissected in cold $HBSS^+$ solution and the meninges were removed. Cortical samples were cut in small pieces and were gently triturated with a fire-polished glass Pasteur pipette in 8 ml $HBSS^+$ solution. The mix was filtered (40 μm filter) and centrifuged at 800 rpm for 8 min. The supernatant was removed and the pellet was dissolved in 2 ml culture medium. Cells were plated on poly-D-lysine (Sigma–Aldrich Chimie, St Quentin Fallavier, France)-coated 12 well (24 mm diameter) plates with glass coverslips (12 mm diameter) (CML, Nemours, France) at a density of 1×10^6 cells/well. Cultures were maintained at 37 °C in a humidified 5% CO_2 atmosphere incubator in Neurobasal supplemented with B27, Glutamax, antibiotics and used for experiments after 16 days. Glial growth was suppressed by addition of 5-Fluoro-2-deoxyuridine (2 μM) and Uridine (2 μM) during the second day of culture. The degree of damage observed in the current *in vitro* system was similar to that previously reported in aging cultures of mouse cortical neurons (Lesuisse and Martin, 2002).

2.2. In vitro model of excitotoxicity

As model of excitotoxicity, we used glutamate at the concentration of 10 μM in magnesium-free glycine-supplemented PBS during 10 min, which induced significant damage as previously reported (Hartley et al., 1993). MLC601 or MLC901 was added at the concentration of 1 μg/ml, 4 days before and after treatment with glutamate. Control cells were incubated with vehicle alone. Cell survival and lactate dehydrogenase (LDH) release were estimated 5, 8 and 24 h after glutamate treatment ($n = 3$ cultures, 36 wells per experimental group).

2.3. Cell injury assay: cell survival and lactate dehydrogenase (LDH) measurements

Cell viability was assessed at Day 8, 10, 12 and 14 of cell culture and at 5, 8 and 24 h after glutamate treatment, by using the Cell Titer 96 (*r*) Aqueous One Solution Cell Proliferation Assay (Promega, Charbonnières-les-Bains, France) ($n = 3$ cultures, 36 wells per experimental group). This assay is a colorimetric method, which is based on the use of the 3-(4,5-dimethylthiazol-2-yl)-5-(3-carboxymethoxyphenyl)-2-(4-sulfophenyl)-2*H*-tetrazolium inner salt (MTS), a marker of mitochondrial activity and an electron-coupling reagent (phenazine ethosulfate, PES). The MTS tetrazolium compound is bioreduced by cells into a colored formazan product that is soluble in tissue culture medium. This conversion is presumably accomplished by NADPH or NADH produced by dehydrogenase enzymes in metabolically active cells. The quantity of formazan product as measured by the absorbance at 490 nm is directly proportional to the number of living cells in culture. According to the manufacturer's recommendations, the assay was performed as follows: the totality of cell culture medium was removed and replaced by 500 μl of Neurobasal medium + Cell Titer 96 Aqueous One Solution. Cells were incubated for 4 h at 37 °C in the humidified 5% CO_2 atmosphere incubator. The reaction was stopped with 2% SDS. Optical density was measured 4 h later at 490 nm utilizing a microplate reader (Labsystem Multiscan RC, VWR International, Fontenay sous Bois, France). Background absorbance at 620 nm was subtracted. Results were expressed in Optical Density ($OD \times 10^{-3}$). To correlate the mitochondrial activity measured by OD in the wells to the cell viability, a calibration curve was performed giving the effect of cell number on absorbance at 490 nm. The correlation coefficient was 0.99, indicating a linear response between cell number and absorbance at 490 nm. Data are expressed as the percentage of cell viability, which is calculated by dividing the absorbance value of MLC601/MLC901-treated samples by that of the untreated controls within each group.

Neuronal injury was quantitatively assessed by the measurement of LDH release from cultured neurons at Day 8, 10, 12 and 14 of cell culture and at 5, 8 and 24 h after glutamate treatment (Day 6 of culture) (Koh and Choi, 1987). LDH release assay provides a measure of cytoplasmic membrane integrity. 100 μl cell culture medium was transferred from culture wells to 96-well plates and mixed with 100 μl reaction solution according to LDH assay kit (Roche Diagnostic: Cytotoxicity Detection). Quantification was done by measuring the Optical Density (OD) 30 min later at 492 nm on a microplate reader (Labsystem Multiscan RC, VWR International, Fontenay sous Bois, France). Background absorbance at 620 nm was subtracted. As recommended by the manufacturer, neurons exposed to a lysis solution (PBS containing 0.1% Triton X-100) were used as positive control and set as 100% LDH release. Data are expressed as ratio of LDH efflux/cell viability.

All *in vitro* experiments were monitored by one researcher blinded to the treatment status ($n = 3$ cultures, 36 wells per experimental group). Results corresponded to the mean of three independent experiments with triplicate determination. Statistical analyses of cell viability and LDH results were assessed using one factor ANOVA test following by post-hoc test ($P < 0.05$).

2.4. Focal ischemia

2.4.1. Animals

All experiments were performed according to policies on the care and use of laboratory animals of European Community legislation. The local Ethics Committee approved the experiments (protocol numbers NCA/2006/10-1 and NCA/2006/10-2). All efforts were made to minimize animal suffering and reduce the number of animals used. Adult male C57/Bl6 mice, weighing 22–26 g (7–9 weeks old) were used in this study. Animals housed under controlled laboratory conditions with a 12-h dark–light cycle, a temperature of 21 ± 2 °C, and a humidity of 60–70% for at least one week prior to drug treatment or surgery. Mice had free access to standard rodent diet and tap water. The researchers, who carried out the ischemic surgery and measured infarct volumes were blinded in regard to the treatment code.

2.4.2. Model of focal ischemia

Ischemia was induced by occlusion of the left middle cerebral artery (MCA) using an intraluminal filament technique (Heurteaux et al., 2006a; Huang et al., 1994). After a midline neck incision was made, the left common and external carotid arteries were isolated and ligated with a 4–0 silk suture thread (Ethicon). A yasargil aneurysm clip (BMH31, Aesculap, Tuttlingen, Germany) was temporarily placed on the internal carotid artery. A 6–0 coated filament (Doccol, Redlands, CA, USA) was introduced through a small incision into the common carotid artery and 13 mm distal to the carotid bifurcation for occlusion of MCA origin. Animals were kept at 37 °C for 1 h, after which time the thread was carefully withdrawn to allow reperfusion of MCA territory. To control MCAO severity regional cerebral blood flow (rCBF) was determined by laser-Doppler flowmetry (Perimed) using a flexible 0.5-mm fiber optic extension to the master probe fixed on the intact skull over the ischemic cortex (2 mm posterior and 6 mm lateral from the bregma). Sham-operation was performed inserting the thread into the common carotid artery without advancing it to occlude MCA. Animals were allowed to regain full consciousness on a heating pad before returning to the cage.

2.4.3. Physiological parameters

General anesthesia was induced with 3% isoflurane and maintained with 1% isoflurane by means of an open facemask for each mouse. Mice were allowed to breathe spontaneously. A subset of animals ($n = 5$ per group) were monitored for physiological parameters including mean arterial blood pressure (MABP), rectal temperature, arterial blood gases and pH before, during and after ischemia. The right femoral artery was catheterized with PE-10 polyethylene tubing and connected to a blood pressure transducer (Harvard Apparatus) for continuous monitoring of MABP (mm Hg). A heparinized blood sample (75 μl) was then obtained from the catheterized femoral artery. Blood P_aO_2, P_aCO_2 and pH were measured using an Acid-Base Laboratory system (ABL 555, Radiometer). Core temperature was continuously monitored with a thermometer (3-mm probe diameter; Harvard Apparatus), inserted into the rectum and maintained at physiological temperatures using a thermostatically controlled heating blanket (Harvard Apparatus). Core temperature was maintained before, during and 3 h after ischemia at physiological values by using the homeothermic blanket control.

2.4.4. Determination of infarct volume

Mice were sacrificed at 30 h after reperfusion. To visualize the evolution and the extent of infarct volume by TTC (2.3.5-triphenyltetrazolium chloride) staining, brains were removed and sectioned into six 1 mm-thick coronal slices using a tissue chopper (Phymep, France). Coronal slices were immediately immersed into 2% TTC (Sigma, France) for 20 min at room temperature in the dark followed by fixation in 4% paraformaldehyde solution overnight prior to analysis (Heurteaux et al., 2006a).

Areas of infarction, outlined in light appeared in white on coronal TTC-stained slices. To confirm the extent of the cerebral lesion, cresyl violet staining on coronal frozen brain sections (10 μm-thick) was performed using a solution of 1% cresyl violet in 0.25% acetic acid and mounted with Entellan. The striatal and cortical areas of infarction, outlined in light were measured on each section using a computer image analysis system and corrected for brain edema according to Golanov and Reis (1995). Infarct volume, expressed in mm^3 was calculated by a linear integration of the corrected lesions areas as previously described (Heurteaux et al., 2006a).

2.5. Drug treatments

MLC601 (NeuroAid) and MLC901 (NeuroAid II) were provided by Moleac (Singapore). The composition of MLC601 (0.4 g per capsule) was the following: 0.57 g Radix astragali, 0.114 g Radix salvia miltiorrhizae, 0.114 g Radix paeoniae rubra, 0.114 g Rhizoma chuanxiong, 0.114 g Radix angelicae sinensis, 0.114 g Carthamus tinctorius, 0.114 g Prunus persica, 0.114 g Radix polygalae, 0.114 g Rhizoma acori tatarinowii, 0.095 g Buthus martensii, 0.0665 Hirudo, 0.0665 g Eupolyphaga seu steleophaga, 0.0285 g Calculus bovisartifactus, 0.0285 g Cornu saigae tataricae. In MLC901, Buthus martensii, Hirudo, Eupolyphaga seu steleophaga, Calculus bovisartifactus and Cornu saigae tataricae have been removed. For *in vitro* experiments, the concentration used in each 24 mm well was 1 μg/ml. A capsule containing 400 mg MLC601 or MLC901 was diluted in 40 ml Neurobasal medium corresponding to a concentration of 10 mg/ml (Stock solution) at 37 °C during 60 min. Cell treatment with MLC601 or MLC901 started at Day 3 of culture during 14 days (corresponding to 17 days of culture). For *in vivo* experiments, MLC901 pre-treatment was given in drinking water at the concentration of 6 mg/ml. One capsule of MLC901 was dissolved in 66 ml water under stirring with an agitator for 1 h at 37 °C. The solution was then filtered with 0.22 μm filter. For *in vivo* post-treatment, mice were intraperitoneally injected with a single dose of 2 μg/ml MLC901 or MLC601 solution diluted in saline (as vehicle) in a total volume of 500 μl/mouse weighing 25 g at the onset of ischemia and 6 h after reperfusion (Post-treatment Onset) or 3 and 24 h following the end of ischemia (Post-Treatment 3H). The dose used for *in vivo* pre-treatment has been selected based on the concentrations used in humans (oral administration: 4 capsules three times a day) (Chen et al., 2009) and reported to the mouse weight and its daily water intake. The dose used in the post-treatment corresponded to the doses used on cortical neurons in culture (see Results Section 3.1). Each treatment group had its own control. The flowchart illustrating the experimental design is given in Fig. 1.

2.6. Motor performance tests

To explore the functional recovery after ischemia, behavioral testing was performed 3 days following ischemia with the rotarod and the actimeter tests, which were monitored by one researcher blinded to mouse treatment code.

2.6.1. Accelerated rotarod

The rotarod test has been used to assess motor coordination and balance alterations after ischemic brain injury in the rodent (Rogers et al., 1997). The rotarod apparatus consists of a striated rod (diameter 3 cm) subdivided into 5 areas (width: 5 cm) by disks 25 cm in diameter. Mice ($n = 10$ per group) were conditioned to the accelerating rotarod (Ugo Basile, France) for three days before MCA occlusion. To this end, mice were first

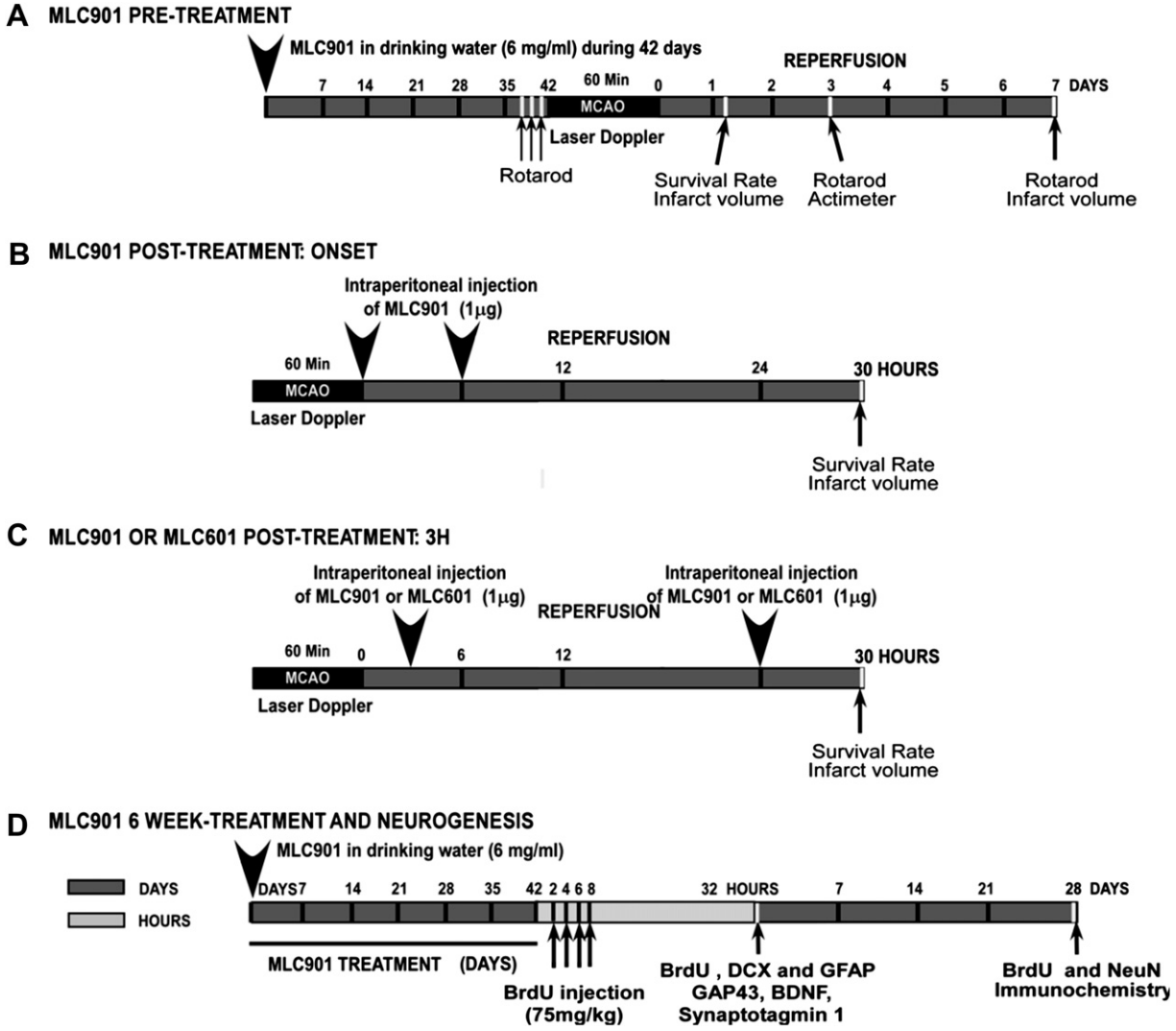

Fig. 1. Flowchart illustrating the different *in vivo* paradigms. In A, B and C, mice were subjected to a 60 min middle cerebral artery occlusion (MCAO). (A) MLC901 pre-treatment administered during 42 days (6 weeks) in drinking water (6 mg/ml). (B) MLC901 Post-treatment: ONSET. MLC01was intraperitoneally injected (1 μg per mouse) at the onset and 6 h after ischemia. (C) MLC901 Post-treatment: 3H. MLC901 or MLC601 was intraperitoneally injected (1 μg per mouse) 3 and 24 h after ischemia. (D) MLC901 pre-treatment and neurogenesis. MLC901 was administered during 42 days (6 weeks) in drinking water (6 mg/ml). 24 h later, mice received 4 BrdU intraperitoneal injections (75 mg/kg) at 2 h interval.

placed on the apparatus during 30 s with no rotation and thereafter for 2 min with a constant low speed (4 rpm). They were tested until they achieved a criterion of remaining on the rotating spindle for 1 min. This procedure was performed only the first day of training. After 10 min rest, each mouse then received a single baseline trial on the accelerating rotarod in which the spindle increased in speed from 4 to 40 rpm over a period of 6 min. The same protocol was applied at Day −3, Day −2 and Day −1. The test trial was performed at Day +3 and Day +7 after MCA occlusion. The maximum duration the animals were able to walk on the rotarod before falling was measured (maximum value: 6 min). The trial was ended if the mice gripped the device and spun around for 2 consecutive revolutions. Mice were tested over three daily trials in the accelerated condition (4–40 rpm). The daily mean value was taken for each mouse and used for statistical analysis.

2.6.2. Spontaneous locomotor activity

Mice were placed individually into an activity-monitoring system (Imetronic, France), consisting of clear plexiglas cages each with 3 banks of photoelectric emitters and detectors. Total locomotor activity *i.e.* quantification of the total number of activity counts (photocell beam breaks) was recorded for 24 h. A locomotor activity test for 24 h was performed before ischemia surgery and three days after MCA occlusion. Total activity corresponded to different movements of animals: coming-and-going between the back and the front of the cage, climbing, and other movements in the back or the front of the cage ($n = 10$ per group).

2.7. Immunohistochemistry on cortical neurons in culture or brain sections

Cortical cells on coverslips or brain sections were fixed with 4% paraformaldehyde/PBS, permeabilized in 0.3% polyoxyethylensorbitan monolaurate (Tween 20, Sigma) for 10 min and blocked with 2.5% donkey serum/PBS for 2 h at room temperature. Cells or sections were incubated with an anti-doublecortin (DCX) antibody (1/200, Santa Cruz SC-8066), a mouse anti-synaptotagmin 1 (1:100, Stressgen, Euromedex), a rabbit anti-GAP43 (1:300, Abcam Limited) or a rabbit anti-mature-BDNF (1/200, Chemicon International, Hampshire, UK) in 2% donkey serum/phosphate buffer saline overnight (Heurteaux et al., 2006b). After 3 washes in phosphate buffer saline (PBS), cells or sections were incubated in anti-goat Alexa-488-coupled antibodies (FluoProbes) in 2% donkey serum for 2 h, washed three times in PBS for 5 min each. Then, neurons were incubated in Hoechst solution (3 μl in 10 ml, Sigma–Aldrich Chimie, Saint Quentin Fallavier, France) for 10 min to label cell nuclei. After 2 washes in PBS and 1 wash in water, coverslips or sections were dried and mounted on glass slides with Fluoroprep (Biomérieux: 75521). Cells or sections were observed using confocal epifluorescence microscopy. Confocal microscopy observations were performed using a Laser Scanning Confocal Microscope (TCS SP, Leica) equipped with a DMIRBE inverted microscope and an argon–krypton laser (laser excitation 488 nm, acquisition 500–600 nm every 10 nm). Signal specificity was assessed in negative control coverslips by omitting primary antibody. Images were acquired as single transcellular optical sections and averaged over at least four scans per frame. Epifluorescence microscopy images of protein labelling were captured with identical time of exposition after spectral correction of the autofluorescence background. Analysis of the fluorescence intensity was performed by using the NIH Image J software (http://rsbwebnih.gov/ij), which allowed to extract the fluorescent intensity levels of cells of each fluorescent image saved as a 16-bit TIFF file ($n = 3$ cultures, 12 wells per experimental group, total 15 fields per condition). Results are given as ratio of mean fluorescence intensity in AU (arbitrary unit)/number of labelled cells ± SEM of three experiments. The differentiated neurites of cortical neurons in culture were observed by DCX immunostaining at Day 14 of treatment. Neurite outgrowth was determined on epifluorescence microscopy by measuring total length of neurites in culture dishes at different times of treatment using a cell photo image and Neurite Tracer Image J software (Pool et al., 2008).

2.8. Analysis of in vivo neurogenesis on brain sections

BrdU treatment consisted of 4 injections (75 mg/kg, i.p. each, 2 h interval). Brains were removed at 24 h after the last injection. Serial sections of paraformaldehyde-perfused-brains were cut (40 μm) throughout the entire hippocampus on a vibratome (Leica). Every sixth section throughout the hippocampus was processed for immunohistochemistry (Heurteaux et al., 2006b) using a monoclonal mouse anti-BrdU (1/200; BD Biosciences, Le Pont de Claix). For BrdU chromogenic immunodetection, sections were then incubated for 1 h in biotin-conjugated species-specific secondary antibodies (diluted1/100, Vector Laboratories), followed by a peroxidase–avidin complex solution according to the manufacturer's protocol. The peroxidase activity of immune complexes was visualized with DAB staining using the VectaStain ABC kit (Vector Laboratories). BrdU-labeled cells of granular and subgranular layers were counted in each section ($n = 8$ mice per group, 8 sections per mouse, 3 independent experiments) at 400× under a light microscope by a blind experimenter. The phenotype of BrdU-positive cells was determined using fluorescent double-labelling with the following antibodies and dilutions: anti-sheep BrdU (1:200, Interchim, Montluçon, France), anti-goat DCX (1/200, Santa Cruz Laboratories, Heidelberg, Germany), anti-mouse NeuN (neuron specific nuclear protein, 1/250, Millipore, St Quentin en Yvelines, France), GFAP (Glial Fibrillary Acidic Protein, 1/250, Dako cytomation, Trappes, France) and secondary antibodies conjugated with Alexa Fluor 488 or 594 (1/1000; Molecular Probes, Leiden, Netherlands). Confocal microscopy observations were performed with a Laser Scanning Confocal Microscope (TCS SP, Leica, Rueil Malmaison, France). Counting of BrdU/DCX and BrdU/NeuN-positive cells were performed on each section ($n = 8$ per group and 8 sections per mouse, 3 independent experiments).

2.9. Human embryonic stem cells (hESC) culture

To assess the effects of MLC901 on human cells, neural progenitors were derived from the SA001 (Cellartis AB, Sweden) embryonic stem cells (hESC) line. Neural rosettes were derived in DMEM-12 enriched with N2/B27, FGF2 (10 ng/ml) and bFGF (10 ng/ml). After 10 days of induction, rosettes were harvested, dissociated and cultured in non-adherent conditions to form large floating rosette clusters. Rosette clusters were gently dissociated and plated on polyornithin (15 μg/ml, Sigma)–laminin (15 μg/ml, Sigma)-coated dishes for enrichment of an adherently growing monolayer of neural precursors (NSC). These culture conditions generated a synchronized and homogenously nestin-positive NSC population that can be frozen and thawed for further differentiation. Cell density was adjusted as required before seeding on 96-well plates. MLC901 was added 6 h after seeding at concentrations varying from 0 to 100 μg/ml, and the experiment was ended after 2 days. Cells were either directly used for counting or fixed for 30 min with 4% paraformaldehyde in phosphate-buffered saline (PBS). For immunohistochemistry, human specific anti-nestin polyclonal antibodies (Millipore, ab5922) were applied for 1 h and revealed with Alexa-488 conjugated goat anti-rabbit IgG (Molecular Probes, A11008). Observations were performed on a Zeiss Axiovert 200 fluorescent microscope.

2.10. Statistical analyses

Data were expressed as mean ± S.E.M. Statistical analysis of differences between groups was performed by using unpaired t test or ANOVA. Where F ratios were significant, statistical analyses were extended and post-hoc comparisons made by using Tukey's test multiple comparison tests. Correlation analyses used Pearson's linear regression. In all analyses, the level of significance was set at $P < 0.05$.

3. Results

3.1. MLC601 and MLC901 protect cortical neurons against death associated with aging in culture

Cortical cells were first exposed to three concentrations of MLC601: 0.1, 0.5 and 1.0 μg/ml from Day 1 until Day 14 of treatment. The doses used were first selected based on a previous study on the anti-inflammatory effects of Radix astragali which constitutes the major component of both MLC601 and MLC901 (Ryu et al., 2008). From these results we then conducted pilot studies using a wide range of MLC601/MLC901 concentrations to search the best protection (data not shown). Cell survival was studied at Day 8, 10 and 14. Fig. 2A shows the dose-response effect of MLC601 treatment. Until Day 8 there was no significant differences in neuronal protection on cells treated with MLC601 concentrations of 0.1–0.5–1.0 μg/ml as compared to control ($P > 0.05$) ($n = 36$ wells per group). The protection induced by 1 μg/ml MLC601 appeared at Day 10 of treatment ($^{*}P < 0.05$ versus control group). At Day 14 the concentration of 1 μg/ml MLC601 induced a significant increase (50%) in neuronal survival as compared to control ($^{**}P < 0.01$ versus control group).

We then compared the protective effects of MLC601 and MLC901 treatments against neurodegeneration of cortical cells over time in culture by using cell viability and LDH measurements. At the concentration of 1 μg/ml, which corresponds to the best results obtained on cell viability with MLC601, both treatments induced, as soon as Day 10 of treatment, a significant increase in neuronal viability as compared to respective controls ($^{*}P < 0.05$, $^{**}P < 0.01$) (Fig. 2B). The highest efficacy of both treatments was observed at Day 14 with ∼48% increase of cell survival ($^{**}P < 0.01$). There was no significant difference of efficacy between MLC601 and MLC901 at the different stages of culture ($n = 36$ wells per group) (Fig. 2B). It is well known that increased cell suffering that leads to cell death is associated with increased LDH release. Compared to respective controls both treatments significantly reduced the ratio LDH release/cell viability after 12 and 14 days of treatment ($^{*}P < 0.05$

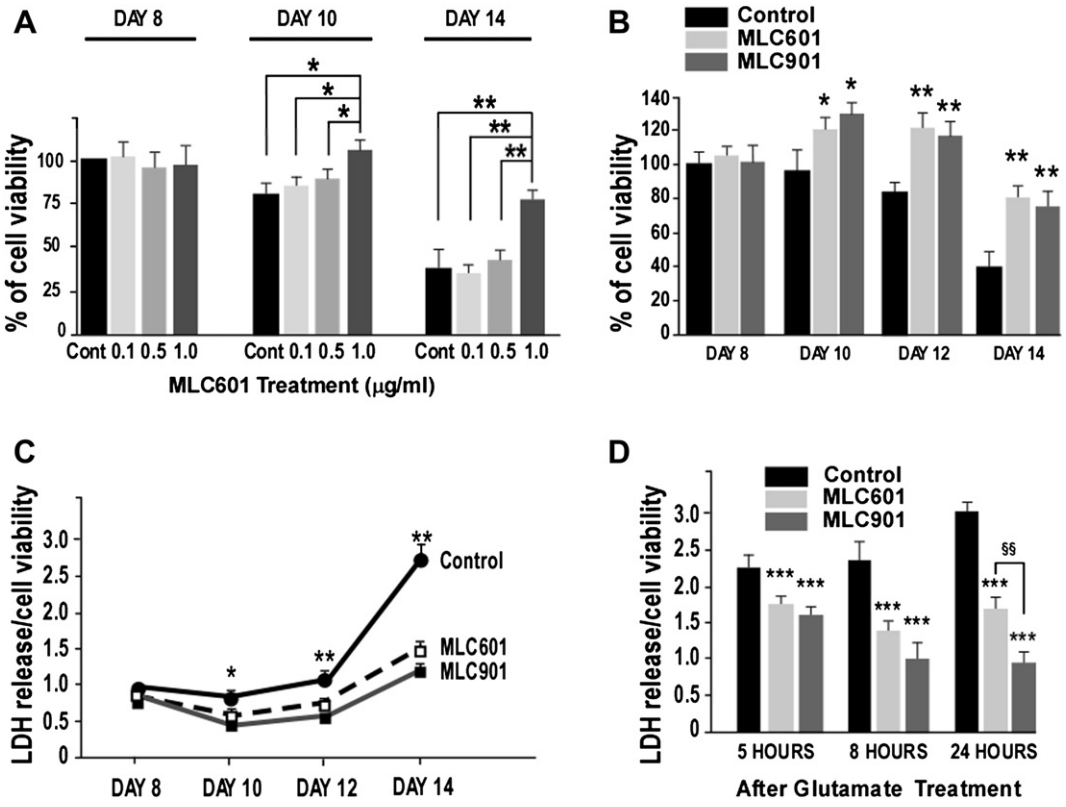

Fig. 2. MLC601 and MLC901 protected cortical neurons in culture. (A) Dose–response effect of MLC601 treatment on cell viability estimated after Day 8, 10 and 14 of treatment ($n = 36$, $^{*}P < 0.05$, $^{**}P < 0.01$ versus control group). (B) Comparative effects between MLC601 and MLC901 treatments (1 μg/ml) on cell viability estimated at Day 8, 10 and 14 of treatment ($n = 36$ wells per experimental group, $^{*}P < 0.05$, $^{**}P < 0.01$ versus control group). (C) Comparative effects between MLC601 and MLC901 treatments (1 μg/ml) on LDH release estimated at Day 8, 10, 12 and 14 of treatment. Results are expressed as ratio of LDH efflux/cell viability ($n = 36$ wells per experimental group, $^{*}P < 0.05$, $^{**}P < 0.01$ versus MLC601 and MLC901 group). (D) Inhibition by MLC601 and MLC901 of LDH release induced by 10 μM glutamate for 10 min. MLC601 or MLC901 at the concentration of 1 μg/ml was added 4 days before and after the treatment with glutamate. Results are expressed as ratio of LDH efflux/cell viability ($n = 12$ wells per experimental group, $^{***}P < 0.001$ versus control group, $^{§§}P < 0.01$ versus MLC601).

and $^{**}P < 0.01$) ($n = 36$ wells per group). There was no significant difference of efficacy on LDH release between MLC601 and MLC901 treatments (Fig. 2C).

3.2. MLC601 and MLC901 protect against glutamate-induced cell death in cortical cultures

Cell injury was estimated by measuring the ratio LDH release/cell viability at various time points (5, 8 and 24 h) after glutamate treatment applied for 10 min in the medium of the primary cortical culture at the concentration of 10 μM. When cortical cells were exposed to 10 μM glutamate, no signs of cell death were observed in the first hours after the exposure. Then, cells died during the next several hours. Application of glutamate on cortical cells during 10 min induced a time-dependent increase in LDH release. Addition of either 1 μg/ml MLC601 or MLC901, 4 days before and after glutamate treatment significantly reduced the ratio LDH release/cell survival (Fig. 2D). For both TCM preparations, the protection was obtained as soon as 5 h and was maintained at 24 h after glutamate. MLC901-induced the best protective effect against excitotoxicity. At 24 h after glutamate treatment for 10 min, the ratio LDH/cell survival decreased from 2.98 to 1.65 with MLC601. It was further decreased to 0.85 with MLC901 (Fig. 2D). Compared to control, half of cortical neurons survived after MLC601/MLC901 treatments. However, MLC901 showed a significant efficacy against glutamate-induced cell death as compared to MLC601 ($^{§§}P < 0.01$).

3.3. Pre- and post-treatments with MLC901/MLC601 protect against ischemic brain injury in vivo

To assay the potential neuroprotective effects of MLC901/MLC601 *in vivo*, we tested the preparation in a mouse model of focal ischemia. Ischemia was induced by transient middle cerebral artery occlusion (MCAO) for 60 min (Huang et al., 1994). We first analyzed whether *a pre-treatment of MLC901* could increase the rate of survival of mice subjected to ischemia and reduce the infarct volume. Animals were first treated with MLC901 administered in the drinking water (6 mg/ml) for 6 weeks before the induction of ischemia. This paradigm corresponds to Fig. 1A. There was no significant difference in the consumption of food and drinking solution between vehicle- and MLC901-treated groups (data not shown). MCAO (60 min) resulted in an infarct in the right MCA perfused region. Fig. 3A shows that a 6 week-pre-treatment of MLC901-induced a marked reduction of the mortality of treated animals, compared to control ischemic mice. MLC901 pre-treatment induced a survival rate of 82% as compared to 65.5% in the control group (Fig. 3A). Representative photographs of stained brain slices at 30 h following ischemia are shown in Fig. 3E. As indicated by the white area on TTC-stained brain slices, cerebral infarcts in MCL901-treated mice were reduced. The infarct spread into the dorsomedial cortex in the MCA region and the caudate-putamen was particularly inhibited by MLC901 pre-treatment (Fig. 3E). The beneficial MLC901 effect was confirmed by the quantitative assessment of total infarct volume on cresyl violet-stained brain sections 30 h following MCAO, which revealed

a significant decrease as compared to sham and ischemic control (Fig. 3B, $^{**}P < 0.01$ versus vehicle group). We then analyzed the potential protection against ischemic stroke induced by an *acute MLC901 post-treatment*. Mice were subjected to focal ischemia and intraperitoneally injected with a single dose of 1 μg of MLC901 solution at the onset of ischemia and again 6 h after reperfusion (Fig. 3C–E: Post-treatment Onset). This paradigm corresponds to Fig. 1B. Acute administration of MLC901-induced a survival rate of 90% compared to 69.5% in ischemic vehicle-treated mice (Fig. 3C). This treatment also drastically decreased cerebral infarction (Fig. 3D and E). MLC901 reduced the stroke volume by 47.2% ($^{**}P < 0.01$) as compared to control ischemic mice at 30 h post-ischemia (Fig. 3D). To analyze whether the time window of protection would allow delayed administration of TCM after stroke, MLC901 was intraperitoneally administered at 3 h and then again at 24 h after MCAO (Post-treatment 3H). This treatment also provided an important protection (Fig. 3C–E). When given as late as 3 and 24 h after the end of ischemia (see paradigm Fig. 1C), the level of survival of MLC901-treated mice remained high (Fig. 3C) and their infarct size was significantly smaller than for vehicle-treated animals after 30 h of reperfusion (Fig. 3D and E, $^{***}P < 0.001$). MCL601 (1 μg, *i.p.*) injected at 3 and 24 h after MCAO (Post-treatment 3 H, see paradigm Fig. 1C) produced beneficial effects on mortality rate (Fig. 3C) and infarct volume (Fig. 3D and E, $^{***}P < 0.01$ versus vehicle group) comparable to those of MLC901 at the same dose and in the same time window ($P > 0.05$). Physiological parameters were carefully measured after 1 h in selected mice ($n = 5$) subjected to MCAO and treated with vehicle versus MLC901 (pre- or post-treatment). Overall, there was no difference in mean arterial blood pressure, P_aCO_2, P_aO_2, pH or rectal temperature after MLC901 administration compared with vehicle-treated animals (Table 1).

3.4. MLC901 pre-treatment protects against functional deficits induced by focal ischemia in vivo

To determine whether a MLC901 pre-treatment before ischemia could have a positive effect on functional recovery after stroke, mice were preventively treated with MLC901 administered in the drinking water (6 mg/ml) during 6 weeks before MCAO occlusion. Then, a first type of functional assessment was carried out 3 and 7 days after stroke using the accelerated rotarod test. There was no significant difference in performance between pre-ischemia groups with or without MLC901 ($P > 0.5$). Three days after MCAO, vehicle-treated mice showed a decrease in their performances as compared to the corresponding pre-ischemia and sham groups ($^{\#\#\#}P < 0.001$). MLC901-treated mice showed a very significant improvement of their performances on the rotarod compared with the vehicle-treated ischemic group (Fig. 4A, $^{***}P < 0.001$). At Day 7 post-ischemia, vehicle-treated mice still displayed a very significant negative difference in the time they could spend on the rod compared to sham-operated and pre-ischemia groups ($^{\#\#\#}P < 0.001$). Interestingly after 7 days, MLC901-treated mice tended to behave in the rotarod assay as well as mice in the pre-ischemia group and as well as, or nearly as well as, the sham group ($^{\$\$}P < 0.01$), again indicating the beneficial effect of MLC901 treatment. To determine whether the functional outcome assessed by measurement of the motor impairment was correlated to the volume of infarction, we quantified at Day 7 post-ischemia the brain damage of mice that underwent the behavioral tests. Fig. 4B shows that there is a significant correlation

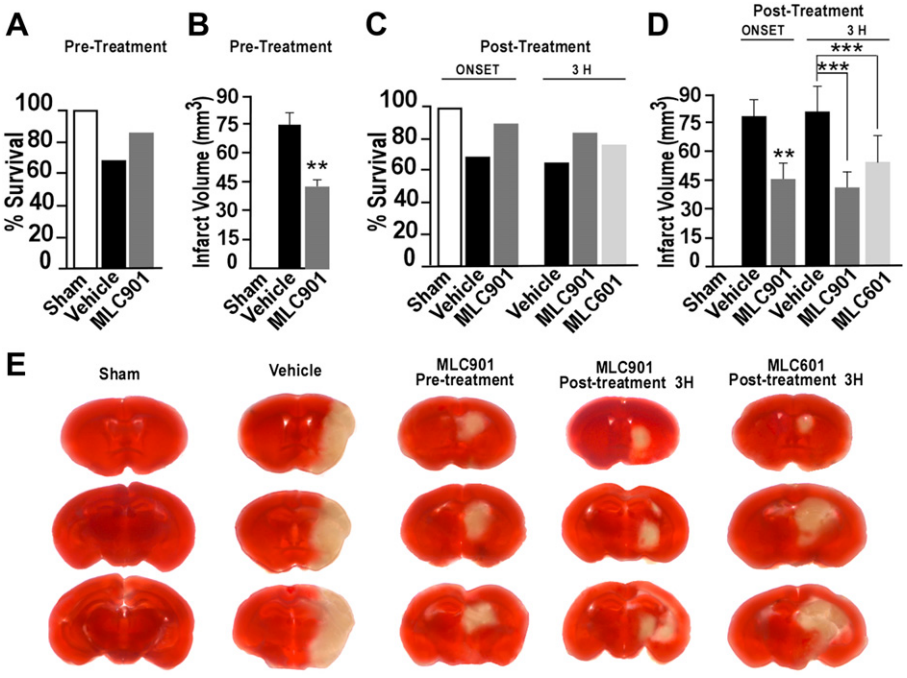

Fig. 3. Pre- and post-treatments with MLC901/MLC601 significantly increased the cerebral protection in a model of focal ischemia *in vivo*. (A–B) Effect of MLC901 pre-treatment on survival rate (A) and infarct volume (B) in mice subjected to 1-h reversible MCAO and killed after 30 h of reperfusion ($n = 25$ per experimental group, $^{**}P < 0.01$ versus water ischemic group). MLC901 pre-treatment was given in drinking water (6 mg/ml) for 6 weeks before the induction of ischemia. (C) Survival rate of mice post-treated with MLC901 or MLC601 and killed 30 h post-MCAO. (D) Infarct volume after MLC901-post-treatment measured at 30 h post-ischemia ($n = 15$ per group, $^{**}P < 0.01$ or $^{***}P < 0.001$ versus respective vehicle-treated ischemic mice). Mice were subjected to focal ischemia and intraperitoneally injected with a single dose of 1 μg of MLC901 solution at the onset of ischemia and 6 h after reperfusion (Post-treatment called ONSET) or injected with MLC901 or MLC601 (1 μg) 3 h after the end of ischemia and 24 h after reperfusion (Post-treatment called 3H). (E) Representative photographs of brain infarction at cortical, hippocampal and striatal levels assessed in each experimental group on seried TTC-stained slices from mice killed 30 h after MCAO. For the survival rate, results are given in percentage of control, corresponding to sham group. For the infarct volume, data are expressed as means ± SEM.

Table 1
Effect of MCAO on physiological parameters in vehicle and MLC901-treated mice.

Parameters	Vehicle	MLC901 pre-treatment	MLC901 post-treatment (1H)
pH	7.29 ± 0.03	7.30 ± 0.02	7.29 ± 0.01
P_aCO_2, mm Hg	39.9 ± 1.2	40.2 ± 1.4	40.7 ± 1.1
P_a0_2, mm Hg	118 ± 6	120 ± 5	117 ± 7
MABP, mm Hg			
Baseline	80 ± 4	83 ± 6	82 ± 5
1 h MCAO	62 ± 5	59 ± 7	61 ± 6
3 h reperfusion	75 ± 4	79 ± 6	78 ± 5
Core temperature (°C)			
Baseline	36.7 ± 0.2	36.9 ± 0.3	36.8 ± 0.3
1 h MCAO	36.8 ± 0.2	36.8 ± 0.2	36.9 ± 0.2
3 h reperfusion	36.7 ± 0.2	36.9 ± 0.3	36.9 ± 0.1

Mice were subjected to 60 min MCAO followed by reperfusion. With MLC901 pre-treatment animals were treated with MLC901 administered in the drinking water (6 mg/ml) for 6 weeks before the induction of ischemia. With MLC901 post-treatment (1H), Mice were subjected to focal ischemia and intraperitoneally injected with a single dose of 1 μg/ml of MLC901 solution at the onset of ischemia and 6 h after reperfusion. MABP (mean arterial blood pressure in mm Hg) was measured before, during and 3 h after ischemia. 50 μl of blood were withdrawn during focal ischemia for blood gas determination (pH, P_aO_2, P_aCO_2). Recta core temperature (in °C) was controlled by using a homeothermic blanket control before, during and 3 h after ischemia.

($r = 0.868$) between performances on the accelerated rotarod and infarct volumes one week after stroke ($F(1.34) = 0.418$, $P = 0.0002$). The spontaneous locomotor activity test confirmed the rotarod results. Again, when tested before MCAO, there was no difference between groups. However, a large difference in behavioral impairment appeared at three days after ischemia. The locomotor activity, including climbing was much higher in MLC901-treated mice than in corresponding vehicle-treated animals (Fig. 4C, $^{*}P < 0.05$, $^{**}P < 0.01$).

3.5. MLC601/MLC901 treatment induces neurogenesis, neuroproliferation, and neurite outgrowth

A focal cerebral ischemia, induced by insertion of a filament in the MCA leads to damage of cortical and striatal brain areas. A "repair" of these damaged areas might be possible by activating endogenous stem cells. It is known that an increase of endogenous cell proliferation occurs in the subgranular zone (SGZ) of dentate gyrus after ischemia (Zhang et al., 2008) as it does after application of different factors such as growth factors (Chen et al., 2003; Sharp et al., 2002). To determine whether MLC901 is able to promote basal neurogenesis, we analyzed incorporation of BrdU (5-bromo-2′-deoxyuridine, a DNA synthesis marker) in dividing progenitor cells, corresponding to the production of newborn neurons, in mice with a 6 week-treatment with MLC901 alone, not followed by an ischemic insult (see paradigm in Fig. 1D) and compared the results with non-treated mice. Fig. 5A shows representative photographs of MLC01 effect on neurogenesis. There was a clear increase of the number of BrdU-labeled cells in the SGZ. MLC901 treatment in the drinking water for 6 weeks resulted in a 1.4-fold increase in the number of BrdU-labeled cells as compared to vehicle-treated animals ($^{***}P < 0.001$). We then provided evidence that proliferating cells were immature neurons. The phenotype of BrdU-positive cells in the SGZ was analyzed by double-labelling with doublecortin (DCX) for neurons and Glial Fibrillary Acidic Protein (GFAP) for astroglia. DCX is a highly hydrophilic microtubule-associated protein that is specifically expressed in migrating neuronal precursors and in areas of continuous neurogenesis in adult brain (Couillard-Despres et al., 2005). Fig. 5B shows representative confocal microscopy images of dual labelling of BrdU and DCX at 24 h following the last injection of BrdU. In contrast, no co-localization of BrdU-positive cells with the astroglial marker GFAP was observed. Counting of BrdU-positive cells (*i.e.* number of new dividing cells) showed that at 24 h following the last injection of BrdU, 72 ± 9% expressed DCX, which identifies immature neurons, in MLC901-treated mice and only 45 ± 5% in the vehicle group (Fig. 5C, $^{***}P < 0.001$) Since newborn cells need about three weeks to differentiate into mature neurons, we then decided to investigate whether the large MLC901-induced increase in neuronal precursors observed at 24 h following the last BrdU injection would correlate with an increase in neuronal maturation as determined by the mature neuron marker NeuN three weeks after the last BrdU injection (Fig. 5B). At this time, counting of BrdU/NeuN^{+} cells showed that MLC901 pre-treatment induced a 2.1-fold increase in the number of mature neurons as compared to vehicle-treated mice (Fig. 5C, $^{**}P < 0.01$).

Neurotrophic factors, and particularly BDNF influence neurogenesis. It is well known that BDNF-mediated pathways are involved in cell survival and plasticity (Aguado et al., 2003; Gorski et al., 2003; Lipsky and Marini, 2007; Mattson, 2008). For this reason, we were curious to see whether MLC901 pre-treatment administered in drinking water for 6 weeks could trigger BDNF expression. Fig. 6A shows *in vivo* effects of MLC901 on BDNF protein levels in cortex sections. A quantitative analysis showed BDNF expression, that was increased 2.46 fold in the cortex of MLC901-treated mice as compared to vehicle group (Fig. 6B, $^{**}P < 0.001$).

At this stage, because the TCM MLC601 has been administered to humans for a long time, it was important to see whether the neurogenic effects of MLC901 could be observed on human ESC-derived progenitors. After 2 days of culture, neural progenitors had displayed a 3-fold increase in number, with a plateau at 250 000 cells for the highest seeding densities. An increase in cell number induced by MLC901 was observed in low-density cultures, and was not observed at higher cell densities (Fig. 7A). Low-density cultures were characterized by spontaneous formation of radiating clusters of nestin-positive progenitors that evoked rosettes (Fig. 7B–D). The number of rosettes was significantly ($^{*}P < 0.05$, $^{**}P < 0.01$) increased by around 3-fold with all indicated concentrations of MLC901 (Fig. 7E).

A more systematic analysis of MLC601/MLC901 effects on neuronal proliferation and neurite outgrowth was then carried out following expression of DCX in the course of time in cultured cortical cells from embryonic mice. Cortical cultures were treated during 14 days and observed at Day 7 and 14 of treatment. In Fig. 8A, representative confocal images of DCX staining show that until Day 7, there is no difference in DCX expression between Vehicle group and cortical cells treated with 1 μg/ml MLC601 or MLC901. However, at Day 14, while DCX immunoreactivity stagnated in Vehicle group, there was a spectacular increase of DCX expression induced by MLC601/MLC901 treatment, highlighting the development of an important axonal and dendritic network. Quantification of the fluorescence intensity in each epifluorescence microscopy image confirmed the neuroproliferative effect of MLC901/601 (Fig. 8B). To investigate whether MLC601/901 treatment could promote neurite outgrowth, we measured the total length of neurites in cultured cortical neurons at Day 14 of treatment. On culture day 1–3 neuronal cells started to aggregate into small clumps. From Day 4, neurons showed developing neurites with increased neurite numbers and size. An analysis of the length of neurites at different times of treatment indicated that neurite outgrowth of cortical cells treated with MLC901 or MLC601 is very significantly increased compared with that of vehicle-treated cells (Fig. 8C, $^{**}P < 0.01$) with a maximum at 8 days of treatment. A similar neurite outgrowth promoting activity was observed for MLC901 and MLC601 ($P > 0.05$).

The effects of MLC601 and MLC901 on expression of the 43 kDa growth-associated protein GAP43 and synaptotagmin 1 at various time points of cortical cultures were also analyzed. GAP43 has an

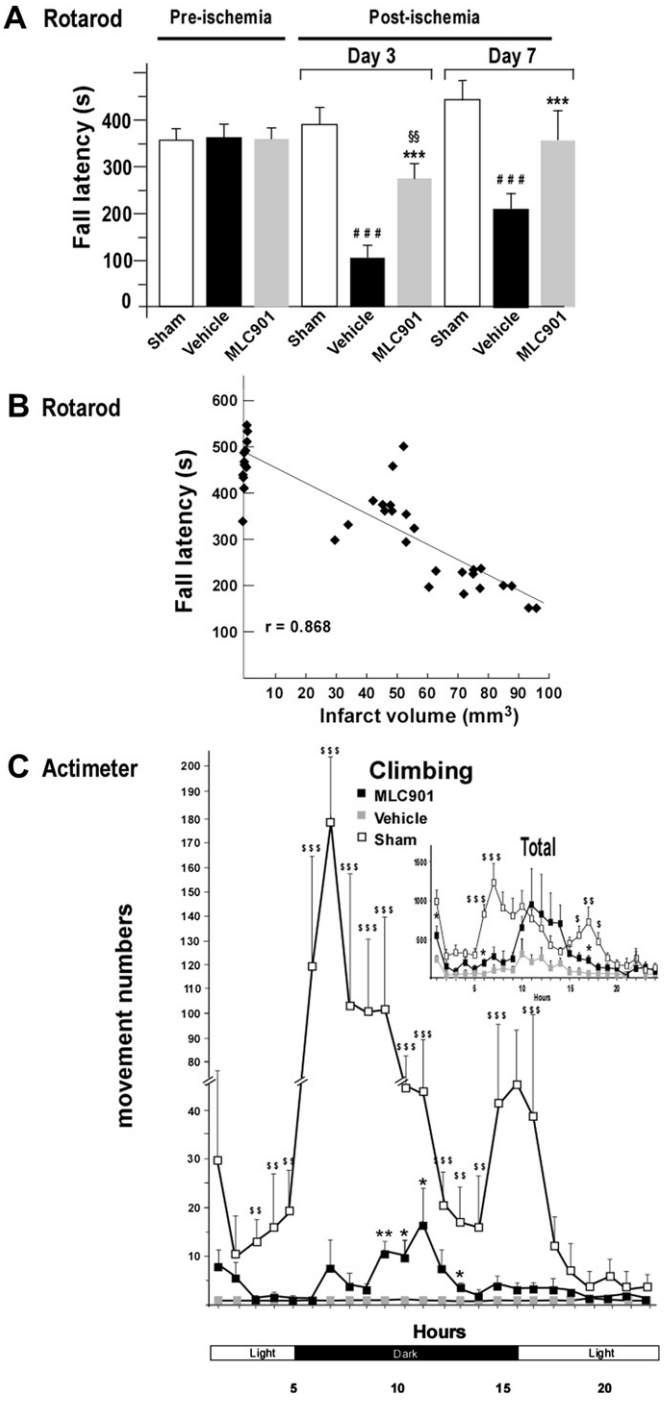

Fig. 4. MLC901 pre-treatment improved functional deficits induced by focal ischemia *in vivo*. (A) MLC901 effect on accelerated rotarod performance (duration spent on rod in seconds) ($n = 12$ per experimental group, $^{***}P < 0.001$ versus vehicle-treated mice, $^{\#\#\#}P < 0.001$ versus pre-ischemia and sham groups, $^{\$\$}P < 0.01$ versus pre-ischemia and sham groups). (B) Correlation between histopathological outcome and motor function 7 days after MCAO. The correlation was obtained from the measure of infarct volumes in the 3 experimental groups (sham, vehicle and MLC901, $n = 12$ per group) and their respective performances on the accelerated rotarod test carried out at day 3 after ischemia. (C) MLC901 effect on spontaneous climbing activity during 24 h, performed 3 days after ischemia. Inset shows the total locomotor activity, including coming-and-going between the back and the front of the cage, climbing, and other movements in the back or the front of the cage ($n = 12$ per group, $^{*}P < 0.05$, $^{**}P < 0.01$, $^{\$\$\$}P < 0.001$ versus vehicle-treated mice). MLC901 was given in drinking water (6 mg/ml) for 6 weeks before the induction of ischemia.

important role in the regulation of neurite outgrowth, growth cone guidance and synaptic plasticity (Van Hooff et al., 1989; Aigner et al., 1995). Immunofluorescent staining of primary cortical neurons with an antibody against GAP43 revealed that this protein was distributed in cytoplasm, membrane and neurite extensions (Fig. 9A). GAP43 expression increased over time in culture both in control and TCM-treated neurons (Fig. 9A). MLC601 and MLC901-treated cortical neurons developed a denser neuritic network, with more frequent elongating neurites and branching, resulting in a relative overgrowth of GAP43 in neurite arborizations compared to vehicle-treated neurons at the same stage. The increase of neurite outgrowth already observed at Day 7 in living neurons was

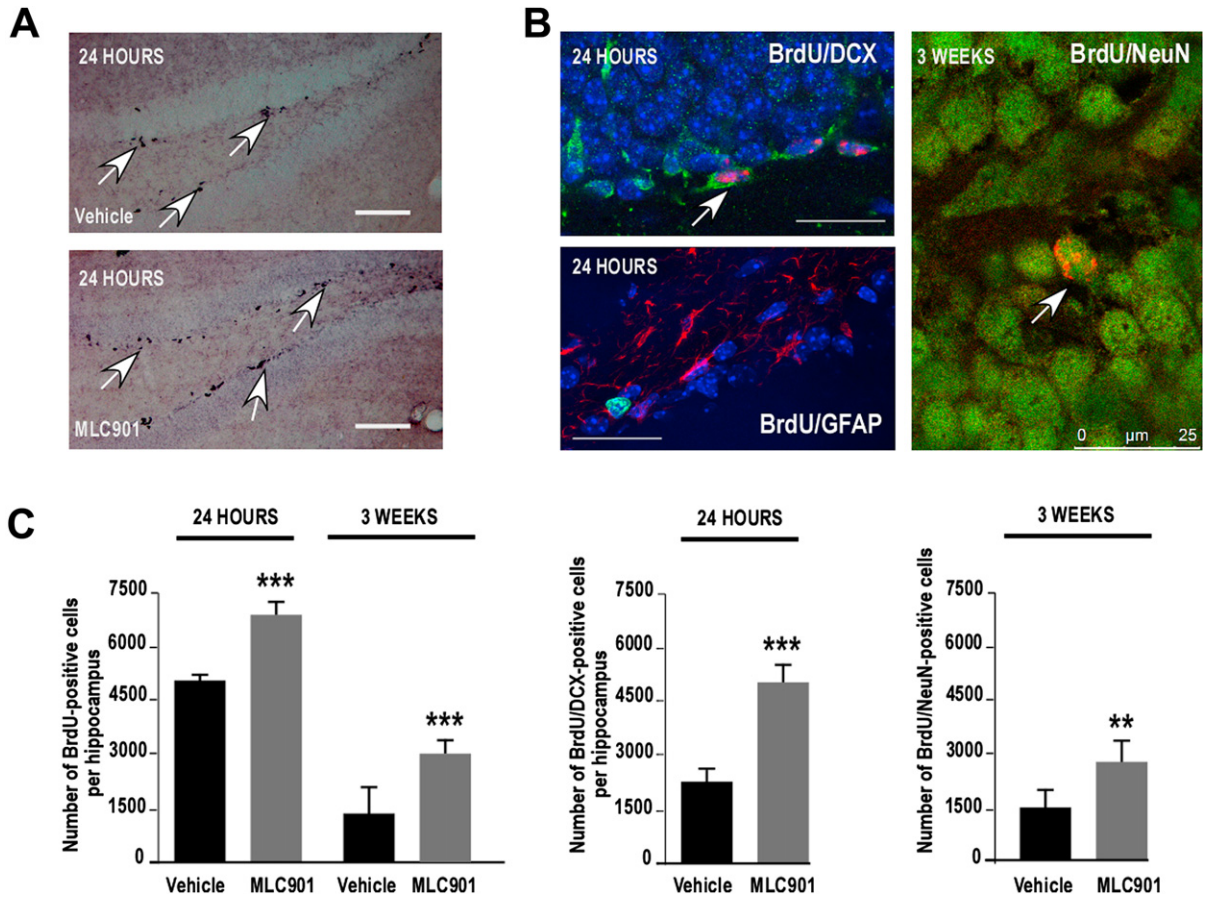

Fig. 5. MLC901 pre-treatment induced neurogenesis and cell proliferation. (A) Representative photomicrographs of BrdU peroxidase-staining (arrows) in dentate gyrus of mouse hippocampus treated for 6 weeks either with vehicle or MLC901. MLC901 treatment was given in drinking water (6 mg/ml). (B) Double-labelling of BrdU-labeled neurons either with DCX, or GFAP 24 h following the last BrdU injection and with NeuN (a neuronal marker) 3 weeks after BrdU. We showed a co-localization only with DCX (neuronal precursor marker in green and BrdU in red labelling), and not with GFAP (glial marker in red and BrdU in green labelling) at 24 h and a BrdU/NeuN co-localization at 3 weeks following BrdU injections (Scale bar, 25 µm) (C) Quantification of BrdU, BrdU/DCX and BrdU/NeuN-positive cells in dentate gyrus treated with vehicle or MLC901 at 24 h and 3 weeks following the last BrdU injection. Data are number of BrdU-positive cells in mouse hippocampus, expressed as mean ± SEM versus vehicle-injected mice. Data were collected in three independent experiments from $n = 8$ per group, 8 sections per group, 10 fields per section, chosen randomly ($^{**}P < 0.01$, $^{***}P < 0.001$ versus vehicle-treated mice).

confirmed and amplified from Day 7 to Day 14. At Day 14, GAP43 was increased 2.2-fold in MLC601- and 2.5-fold MLC901-treated neurons as compared to control neurons ($^{**}P < 0.01$). There was no significant difference between MLC601 and MLC901 (Fig. 9B).

Developing neurons are engaged in neurite outgrowth as well as the synthesis and transport of proteins involved in synaptic transmission. Synaptotagmin 1 is one of synaptic vesicle proteins having a critical role in synaptogenesis and synapse function (Jessell and Kandel, 1993; Sudhof, 1995). It therefore appeared of interest to study the effects of MLC601 and MLC901 treatments at Day 7 and 14 on synaptotagmin 1 expression in cortical neurons in culture. Fig. 10 shows again that cortical neurons underwent a well-defined program of differentiation, including expression of neurite extension and also synapse formation visualized by the expression of

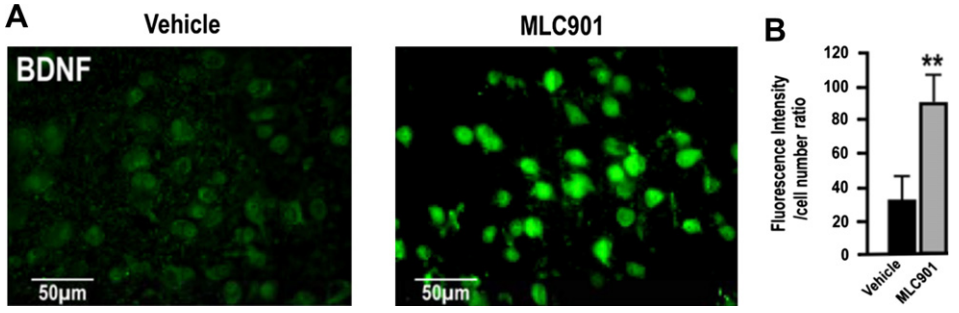

Fig. 6. *In vivo* effect of MLC901 pre-treatment on BDNF protein levels in cortex sections. (A) Representative epifluorescence microscopy photographs of BDNF immunoexpression in cortical neurons in brain sections. (B) Quantification of BDNF signal intensity in immunostained neurons. Data are expressed as ratio of mean fluorescence intensity in AU (arbitrary unit × 1000) to number of labeled cells ± SEM of three experiments. Average fluorescence intensity was expressed from two independent experiments ($n = 8$ sections per experimental group, 15 fields per section and analyzed in triplicate) ($^{**}P < 0.01$ versus vehicle group).

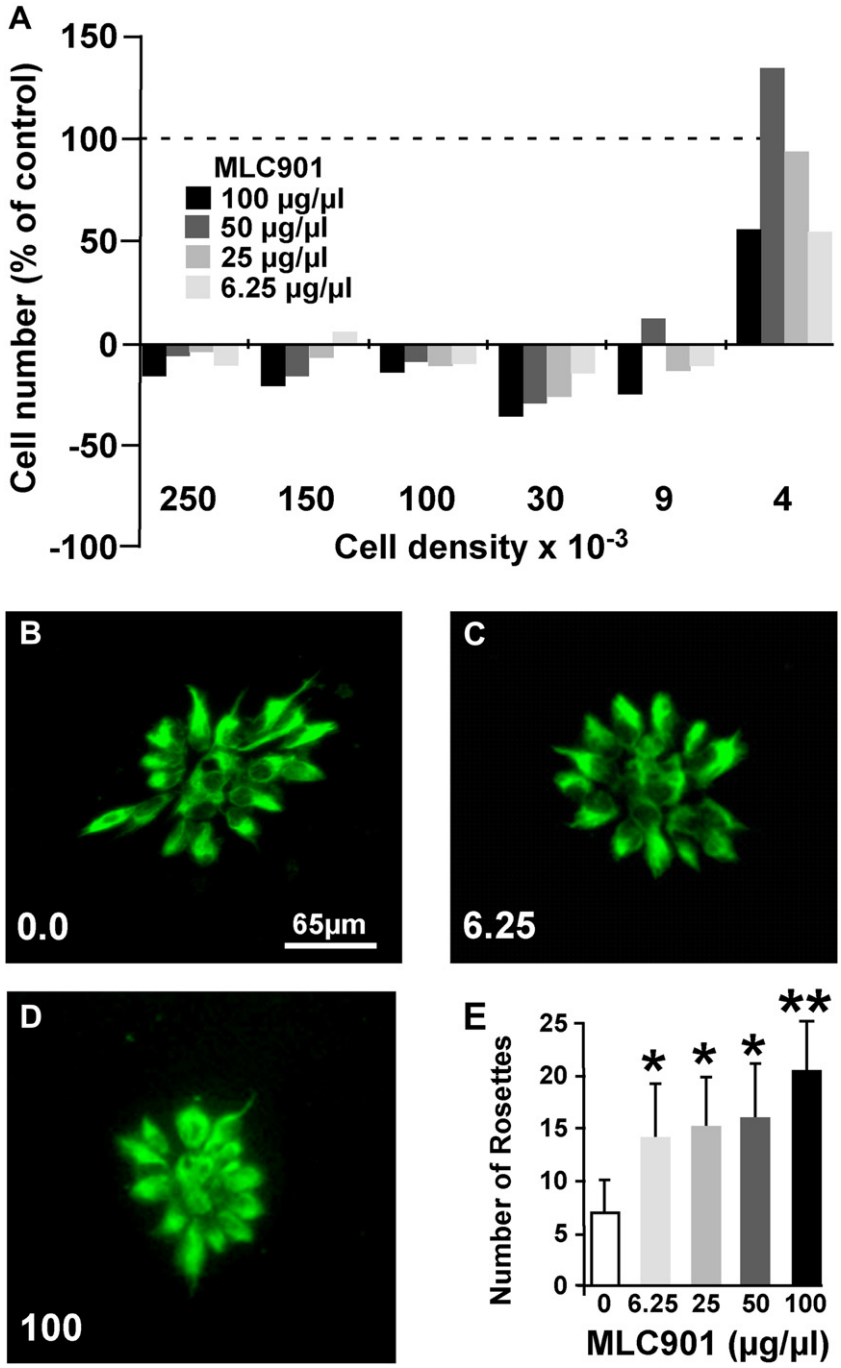

Fig. 7. Neurogenic effects of MLC901 on human ESC-derived progenitors. (A) Effects of MLC901 as a function of cell density. hESC-derived neural progenitors were plated with increasing cell density and were treated with a range of MLC901 concentrations. Cell numbers are expressed as percentage of the control (no treatment, quoted as 0). Increased cell numbers were observed in low-density cultures, with maximal effects for the 50 µg/ml concentration. (B–C–D) Radiant rosette-like aggregates of nestin-positive neural progenitors spontaneously form in low-density cultures (B: no treatment; C: 6.25 µg/ml; D:100 µg/ml). (E) Quantification of the number of rosettes 2 days after the addition of MLC901. ($^{*}P < 0.05$, $^{**}P < 0.01$ versus control).

synaptotagmin 1, which increased with time in culture in the three experimental groups (Fig. 10A). While synaptotagmin 1 immunoreactivity was localized primarily to the soma with a diffuse staining throughout neuritic processes in 4 day-old cultures (data not shown), the staining profile became strikingly different at the 7 and 14 days of treatment with the appearance of intense punctuate staining along neuritic processes, which is characteristic of synaptic release sites in neurons (Fig. 10A). Quantitative analysis of fluorescence intensity in vehicle and MLC601/MLC901-treated cultures showed that both MLC601 and MLC901 treatments significantly increased the levels of synaptotagmin 1, by 1.9 and 2.2-fold respectively, as compared to control cultures ($^{*}P < 0.05$, $^{**}P < 0.01$). MLC901 appears to be slightly more potent than MLC601 (Fig. 10B, $^{\#}P < 0.05$).

4. Discussion

The development of neuroprotective and neurorestorative drugs is essential for the treatment or management of ischemic stroke.

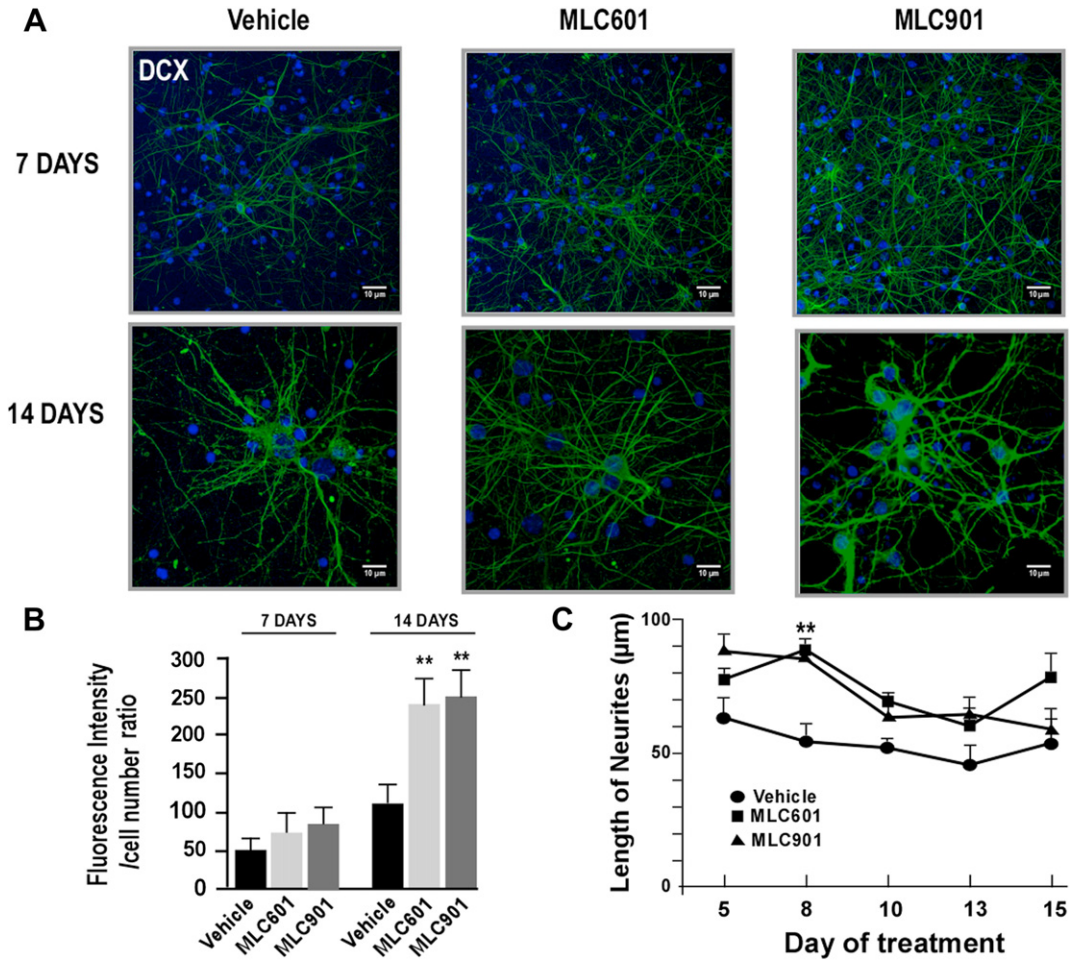

Fig. 8. Effects of MLC601 and MLC901 treatments on *in vitro* DCX immunoexpression in cultured cortical cells. DCX expression was analyzed after MLC601/MLC901 treatments (1 μg/ml) at Day 7 and 14 of treatment. (A) Representative confocal microscopy photographs of DCX expression in cortical neurons stained with anti-DCX antibody. Nuclei were stained with Hoecht 33342 (in blue labelling). (B) Quantification of DCX signal intensity in immunostained neurons observed in epifluorescence microscopy. Data are expressed as ratio of mean fluorescence intensity in AU (arbitrary unit × 1000) to number of labeled cells ± SEM of three experiments. Average fluorescence intensity was expressed from three independent experiments ($n = 12$ wells, 15 fields per well for each experimental group and analyzed in triplicate). (C) Neurite outgrowth obtained by measuring on epifluorescence microscopy the total length of neurites (μm) in function of time of MLC901 and MLC601 treatments. Values are mean ± SEM of three experiments with triplicate ($n = 12$ wells, 15 fields per well for each condition) ($^{**}P < 0.01$ versus vehicle group).

Despite considerable recent progress defining cellular and molecular responses of brain to ischemia, there is no effective treatment for stroke patients besides fibrinolysis at hyper acute stage, and secondary prevention treatments to manage the well identified risk factors. Clinical use of potential neuroprotective treatments has been prevented owing to inefficiency or/and serious side effects caused by their interference with normal brain function (Ginsberg, 2008; Wahlgren and Ahmed, 2004). In an overall research of stroke therapies, whose goal is not only to salvage acutely threatened neuronal tissue but also to promote repair and restoration of function (Martinez-Vila and Irimia, 2005), we have focused our studies on MLC601/MLC901. MLC601 originates from traditional Chinese medicine and MLC901 is a simplified version of MLC601. Traditional Chinese medicine is currently attracting a lot of interest (Wang et al., 2008), particularly in diseases that are not adequately treated with Western medicine. MLC601 is prescribed in several countries of Asia and Middle East. It can be used on top of usual medications, including anti-platelets or anticoagulants. It does not seem to have significant side effects (Gan et al., 2008). Recent trials of MLC601, analyzed in China and Singapore demonstrated beneficial effects on the recovery of independence and motor function after stroke (Chen et al., 2009; Siow, 2008). In regard to these encouraging results, a multicenter clinical trial, called CHIMES is ongoing in Asia (Venketasubramanian et al., 2009).

The purpose of this work was to analyze whether MLC601 and its simplified version MLC901 have any effects on neurogenesis, on the development of the axonal and dendritic network and in neuroprotection, with the idea that positive answers to these questions would also be a strong encouragement to pursue the development of clinical investigations. We demonstrate that MLC901 treatment, when administered *in vivo* in pre- or post-treatments improved animal survival as well as functional neurological recovery and decreases neurodegeneration without affecting physiological parameters. In this work, we used C57Bl/6J mice, a strain known to have an increased vulnerability to focal and global ischemia with a higher level of mortality in comparison to other strains such as DBA/2, MF1 and 129/Sv (Connolly et al., 1996; Fujii et al., 1997). The gain of an important cerebral protection with MLC901 in the suture model of focal ischemia is a strong argument in favor of MLC901 efficiency. Using cortical cells in 17 day-old culture (corresponding to 14 days of treatment), we observed that both MLC901 and MLC601 induced a strong protective effect against glutamate-induced cell death that

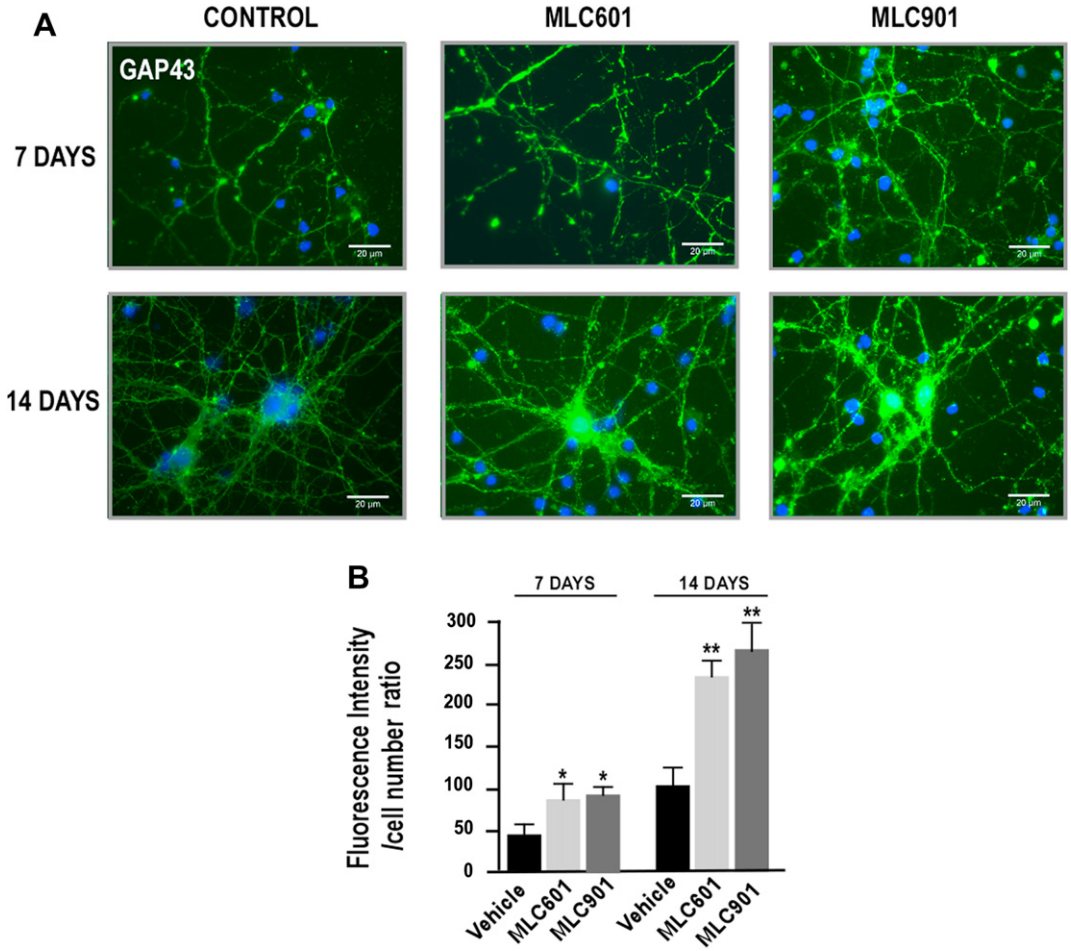

Fig. 9. Effects of MLC601 and MLC901 treatments on *in vitro* GAP43 immunoexpression in cultured cortical neurons. GAP43 expression was analyzed after MLC601/MLC901 treatment (1 µg/ml) at Day 7 and 14 of treatment. (A) Representative photographs of GAP43 expression in epifluorescence microscopy on cortical neurons stained with anti-GAP43 antibody. Nuclei were stained with Hoecht 33342 (in blue). (C) Quantification of GAP43 signal intensity in immunostained neurons. Data are expressed as ratio of mean fluorescence intensity in AU (arbitrary unit × 1000) to number of labeled cells ± SEM of three experiments. Average fluorescence intensity was expressed from three independent sets of experiments ($n = 12$ wells, 15 fields per well for each experimental group and analyzed in triplicate). $^{*}P < 0.05$, $^{*}P < 0.01$ versus vehicle group, Mann–Whitney test.

was maintained 24 h after the excitotoxic injury. It is well known that excessive synaptic glutamate concentration produces excitotoxicity that leads to neuronal death in both global and focal ischemia (Choi, 1998; Obrenovitch et al., 2000). In our *in vivo* model of focal ischemia we clearly demonstrated that MLC601 and MLC901 significantly protected the brain against an ischemic insult. Both pre-treatments administered in drinking water and post-treatment administered intraperitoneally decreased the mortality rate as well as the infarct volume. Therefore, MLC601/MLC901 might be useful as a preventive therapy or as a postischemic treatment to reduce the damaging effects of stroke. MLC601/MLC901 has a time window of protection compatible with clinical trials, since MLC901 provided protection from focal ischemia in the mouse when given as late as 3 h after ischemia. It is interesting to note that MLC601 has the same kind of efficacy *in vivo* since MLC601 post-treatment up to 3 h after stroke also improved survival and protected the brain from ischemic injury.

Until now, the majority of preclinical studies traditionally focused on the prevention of neuronal cell death and attempts to assess behavioral deficits arising from stroke were few, particularly in mice. The ability to demonstrate an improvement of function impaired by ischemia is as important as, and clinically more relevant, than a simple statement of lesion volume. At this stage, it was essential to show that MLC901 protection was accompanied in surviving animals by a decrease of behavioral deficits. In line with first clinical trials that have shown promising results of MLC601 efficiency on the functional recovery after stroke (Chen et al., 2009; Siow, 2008), this work shows that MLC901 improved motor performances measured in the accelerated rotarod and actimeter tests, considered as useful operant conditioning procedures to assess long-lasting deficits after stroke (Ferrara et al., 2009). We focused on the accelerated rotarod test, which provides quantitative, objective and reproducible measures of functional impairment of mice following an ischemic insult. We observed that ischemia-induced impairments with and without MLC901 are directly correlated with the infarct volume: The smaller the infarct volume after MLC901, the higher the level of performance in the rotarod test. The linear relationship between the histopathological outcome and the motor function provides convincing information concerning the use of MLC901 in stroke treatment. These results suggest that MLC901 both preserve damaged neurons and probably at least partially restores neuronal circuits with associated behavioral benefits.

Whereas recovery, in the first few days after stroke, results from edema resolution and/or from reperfusion of the ischemic penumbra, a large part of the recovery over periods of weeks or months is due mainly to brain plasticity, *i.e.* to reorganization of surviving central nervous system elements, probably including stem cells, in the damaged areas (Chopp et al., 2009). Neural plasticity probably involves modulation of signal transduction pathways and regulation

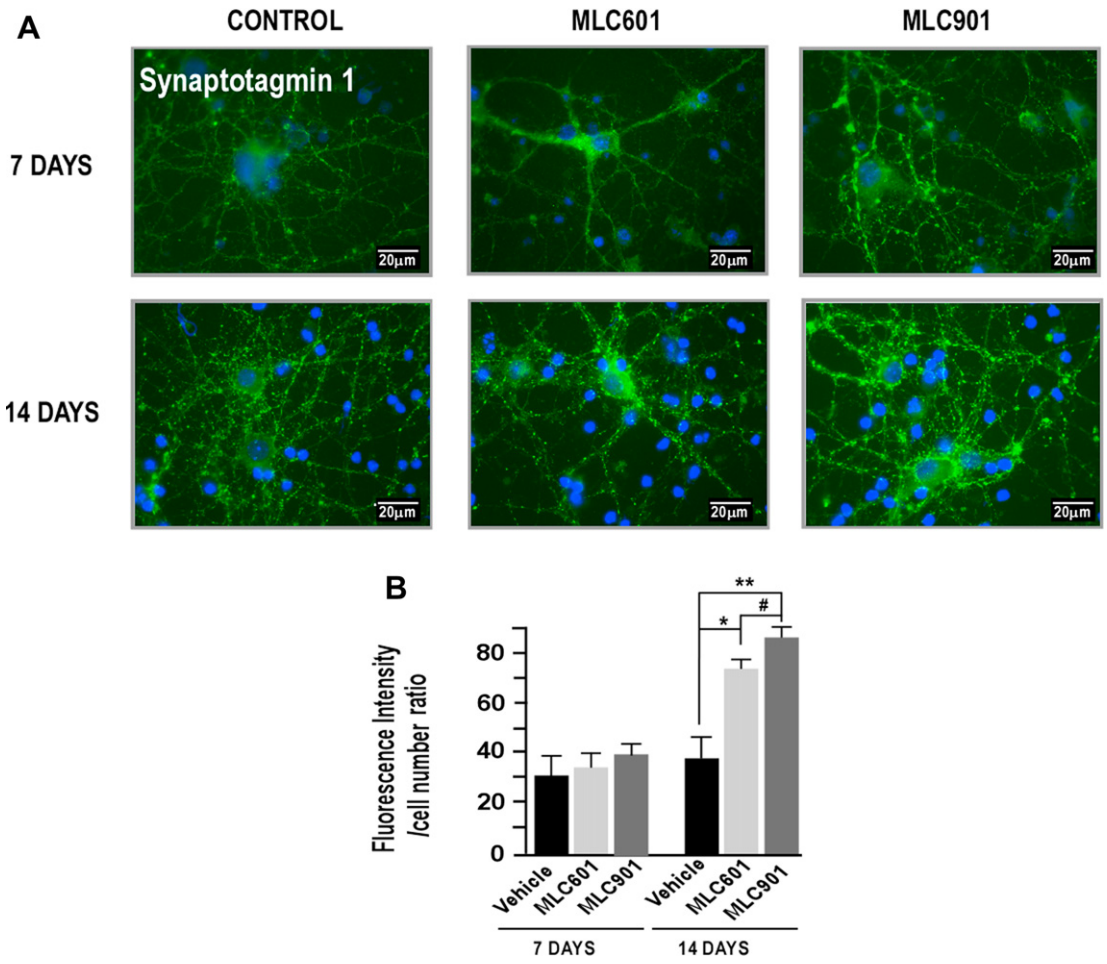

Fig. 10. Effects of MLC601/MLC901 treatment on *in vitro* Synaptotagmin 1 expression in cultured cortical neurons. Synaptotagmin 1 expression was analyzed after MLC601/MLC901 treatment (1 µg/ml) at Day 7 and 14 of treatment. (A) Representative photographs of Synaptotagmin 1 expression in epifluorescence microscopy on cortical neurons stained with anti-Synaptotagmin 1 antibody. Nuclei were stained with Hoecht 33342 (in blue). (C) Quantitation of Synaptotagmin 1 signal intensity in immunostained neurons. Data are expressed as ratio of mean fluorescence intensity in AU (arbitrary unit × 1000) to number of labeled cells ± SEM of three experiments. Average fluorescence intensity was expressed from three independent experiments ($n = 12$ wells, 15 fields per well for each experimental group and analyzed in triplicate). $^{*}P < 0.05$, $^{**}P < 0.01$ versus vehicle group, $P < 0.05$ versus MLC601 group, Mann–Whitney test.

of gene expression as well as neurogenesis, and synaptogenesis. After stroke, the brain uses its complement of neural plastic responses to reorganize, at least partially the cortical maps (Chopp et al., 2009; Di Filippo et al., 2008). Changes in cortical organization include an increase in the number and density of dendrites and synapses. Robust experimental evidence supports the hypothesis that neuronal aggregates adjacent to a lesion in the sensorimotor brain areas can take over progressively the function previously played by the damaged neurons (Zhang et al., 2004). This reorganization subtends clinical recovery of motor performance and sensorimotor integration after stroke. Brain functional imaging studies have shown that recovery from hemiplegic strokes is associated with a marked reorganization of the activation patterns of specific brain structures (Nelles et al., 1999). On the other hand, stroke is known to induce neuronal proliferation associated with directed migration of nascent neurons towards ischemic lesions (Jin et al., 2003). Experimental stroke in adult rodents has been shown to trigger neurogenesis in neuroproliferative zones such as the subgranular zone of dentate gyrus (Sharp et al., 2002). These stroke-activated endogenous neuronal progenitors can migrate into regions that do not normally exhibit neurogenesis in the adult. This raises the possibility that these cells may constitute a pool for the replacement of dead or dysfunctional cells after an ischemic episode. The newly born cells generated from the dentate gyrus develop into granule neurons and are capable of extending axonal projections to the CA3 area and integrating into functional circuits (Hastings and Gould, 1999; Markakis and Gage, 1999). Pharmacological agents able alone to promote basal neurogenesis and synaptogenesis are needed to amplify the intrinsic brain properties for neuroplasticity and subsequent neurological recovery after stroke. In preclinical studies, several potential therapeutic agents have been shown to promote functional outcome after stroke. Most of them are growth factors such as the vascular endothelial growth factor (VEGF), the basic fibroblast growth factor (bFGF), and the brain-derived neurotrophic factor (BDNF) (Chen and Chopp, 2006). Our data show that MLC901 treatment administered for 6 weeks in the drinking water (6 mg/ml) significantly increased the number of BrdU-positive cells in the SGZ, suggesting that this type of medicine could promote basal neurogenesis in the adult brain and play a role in neurologic function recovery of both motor and cognitive functions after stroke. In addition, we report in our *in vitro* experiments with cultured cortical cells that both MLC901 and MLC601 helped to develop a dense axonal and dendritic arborization illustrated by a large increase of DCX fluorescent labelling intensity as well as an enhanced neurite outgrowth. DCX protein is currently used as a classical marker for neurogenesis (Couillard-Despres et al., 2005). DCX appears to be important for the normal developmental

migration of cortical neurons, because mutations in DCX in humans lead to syndromes characterized by migrational arrest of these neurons and manifested clinically by subcortical laminar heterotopias, mental retardation and seizures (des Portes et al., 1998). Increased DCX expression is then closely associated with neurogenic processes.

MLC901-induced neurogenic processes in cortical neurons have also been observed in hESC. MLC901 had a positive effect on the number of neural progenitors derived from hESC, indicating either a neuroprotective effect or an accentuation of proliferation. This effect was observed in low-density cultures, suggesting that cell contact may decrease the action of MLC901. In low-density cultures, hESC spontaneously reconstituted radiating clusters of cells similar to rosettes. Rosettes are radially organized columnar epithelial cells that typically form during differentiation of hESC towards the neural lineage (Elkabetz et al., 2008; Zhang et al., 2001). Progenitors within rosettes differentiate into neurons, astrocytes and oligodendrocytes through a sequence similar to the one observed during neurogenesis. Cell clustering within rosettes reproduces a developmental niche that influences proliferation and differentiation (Illes et al., 2009). Our observations suggest that MLC901 contains key molecules able to create a neurogenic niche and enriched microenvironment to promote amplification and differentiation of neural progenitors.

In order to better decipher the effects of MLC901 and MLC601 on cortical plasticity, we also studied *in vitro* how they modulate the expression of GAP43, associated with neuronal neurite growth and synaptotagmin 1, associated with synapse formation. GAP43 is a membrane-bound protein found in the growth cones of sprouting CNS axons (Aigner et al., 1995; Meiri et al., 1986; Oestreicher et al., 1997; Van Hooff et al., 1989). GAP43 regulates G_o, a GTP-binding protein that transduces information from transmembrane receptors and that is a major component of the neuronal growth cone membrane (Strittmatter et al., 1990). By blocking GAP43 expression with antisense oligonucleotide probes, neurite outgrowth can be eliminated in cultured neurons (Zuber et al., 1989). Synaptotagmin 1 is one of presynaptic vesicle proteins having a critical role in synaptogenesis and synapse function (Jessell and Kandel, 1993; Sudhof, 1995). Synaptotagmin 1 immunostaining is often used to estimate increases or decreases in synaptic numbers. This work reports a significant increase in density of both GAP43 and synaptotagmin 1 in cultured cortical neurons treated with MLC901 compared to vehicle-treated neurons. These data clearly indicate that neurite outgrowth followed by synaptogenesis in cortical neurons is increased by MLC901 treatment. While the specific mechanism responsible for MLC901-promoted expression of proteins involved in neurite growth and synaptogenesis is not yet elucidated, the up-regulation of such proteins classically associated with neuronal remodeling might well explain the enhanced behavioral recovery reported in stroke patients treated with this Chinese medicine (Chen et al., 2009; Siow, 2008) and also in our *in vivo* model of focal ischemia (this work).

One possible mechanism of MLC601/MLC901 effect includes its ability to stimulate BDNF secretion. BDNF is a growth factor which regulates neuronal survival and protect neurons from glutamate-induced damages (Mattson, 2008). BDNF has multiple effects on sustaining and evoking elements of brain plasticity including neurite outgrowth and differentiation (Aguado et al., 2003; Gorski et al., 2003; Volosin et al., 2006). BDNF induction is both spatially and temporally associated with recruitment of new neurons (Mattson, 2008). Our *in vitro* data show that MLC901 indeed increased BDNF expression in cortical neurons. On the other hand GAP43, whose expression is itself increased by MLC901 and MLC601 is known to be essential for the neurotrophic effects of BDNF (Gupta et al., 2009). BDNF is known to also induce anti-apoptotic mechanisms after stroke and reduce infarct size and secondary neuronal cell death (Schabitz et al., 2000; Zhang and Pardridge, 2001). All these data suggest that BDNF may play a significant role in the many beneficial effects displayed by MLC901. In addition, Radix astragali, which is the major component of MLC901/MLC601 herb mixture, has been reported to scavenge active oxidants, and regulate the expression of cytokines such as TNFα, IL-1a, IL-1b, IL-6 as well as the production of nitric oxide (NO), which are all involved in the pathophysiology of stroke (Lee et al., 2005). All these interesting effects induced by Radix astragali alone could of course contribute to the beneficial effects of MLC901/601 against stroke.

Brain injury following stroke results from the complex interplay of multiple pathways including excitotoxicity, acidosis, ionic balance, peri-infarct depolarization, oxidative stress, inflammation and apoptosis (Doyle et al., 2008). It is highly probable that MLC901/MLC601 have "multi-target" effects, which will have to be investigated in details in the near future. MLC901/MLC601 contains a complex mixture of natural molecules that are probably acting in an additive way or in synergy, as recently reported for another TCM treatment against promyelocytic leukemia (Wang et al., 2008).

This work represents the first preclinical study demonstrating neuroprotective and neuroproliferative effects of two natural preparations MLC601 and MLC901, which are already used for the treatment of patients against the deleterious effects of stroke, particularly in Asia. It provides scientific support for their clinical use (i) preventively in patients at high risks to have stroke, (ii) curatively for stroke patients, immediately after stroke, (iii) as it is the case at the present time (Chen et al., 2009) after some weeks or some months after stroke to increase chances to recover better neurological functions. Given the near absence of effective treatments today, the results of the multicenter CHIMES study, which is ongoing in Asia (Venketasubramanian et al., 2009) to more systematically test MLC601 efficacy in humans in a 72 h time window post-stroke onset will be awaited.

Acknowledgments

The authors are very grateful to Dr M. Vasseur for suggesting the project and to D. Picard (Moleac Singapore) for helpful and inspiring discussions concerning the present evaluation of the clinical effects of MLC601 and for both providing MLC601 and MLC901 capsules. This work is supported by the Centre National de la Recherche Scientifique (CNRS), the Fondation de la Recherche Médicale (FRM) and the Association Française contre les Myopathies (AFM).

References

Aguado, F., Carmona, M.A., Pozas, E., Aguilo, A., Martinez-Guijarro, F.J., Alcantara, S., Borrell, V., Yuste, R., Ibanez, C.F., Soriano, E., 2003. BDNF regulates spontaneous correlated activity at early developmental stages by increasing synaptogenesis and expression of the K^+/Cl^- co-transporter KCC2. Development 130, 1267–1280.

Aigner, L., Arber, S., Kapfhammer, J.P., Laux, T., Schneider, C., Botteri, F., Brenner, H.R., Caroni, P., 1995. Overexpression of the neural growth-associated protein GAP-43 induces nerve sprouting in the adult nervous system of transgenic mice. Cell 83, 269–278.

Chen, J., Chopp, M., 2006. Neurorestorative treatment of stroke: cell and pharmacological approaches. NeuroRx 3, 466–473.

Chen, J., Zhang, Z.G., Li, Y., Wang, Y., Wang, L., Jiang, H., Zhang, C., Lu, M., Katakowski, M., Feldkamp, C.S., Chopp, M., 2003. Statins induce angiogenesis, neurogenesis, and synaptogenesis after stroke. Ann. Neurol. 53, 743–751.

Chen, C., Venketasubramanian, N., Gan, R.N., Lambert, C., Picard, D., Chan, B.P., Chan, E., Bousser, M.G., Xuemin, S., 2009. Danqi Piantan Jiaonang (DJ), a traditional Chinese medicine, in poststroke recovery. Stroke 40, 859–863.

Choi, D., 1998. Antagonizing excitotoxicity: a therapeutic strategy for stroke? Mt. Sinai J. Med. 65, 133–138.

Chopp, M., Li, Y., Zhang, Z.G., 2009. Mechanisms underlying improved recovery of neurological function after stroke in the rodent after treatment with neurorestorative cell-based therapies. Stroke 40, S143–S145.

Connolly Jr., E.S., Winfree, C.J., Stern, D.M., Solomon, R.A., Pinsky, D.J., 1996. Procedural and strain-related variables significantly affect outcome in a murine model of focal cerebral ischemia. Neurosurgery 38, 523–531 (discussion 532).

Couillard-Despres, S., Winner, B., Schaubeck, S., Aigner, R., Vroemen, M., Weidner, N., Bogdahn, U., Winkler, J., Kuhn, H.G., Aigner, L., 2005. Doublecortin expression levels in adult brain reflect neurogenesis. Eur. J. Neurosci. 21, 1–14.
Cramer, S.C., 2008. Repairing the human brain after stroke: I. Mechanisms of spontaneous recovery. Ann. Neurol. 63, 272–287.
des Portes, V., Francis, F., Pinard, J.M., Desguerre, I., Moutard, M.L., Snoeck, I., Meiners, L.C., Capron, F., Cusmai, R., Ricci, S., Motte, J., Echenne, B., Ponsot, G., Dulac, O., Chelly, J., Beldjord, C., 1998. Doublecortin is the major gene causing X-linked subcortical laminar heterotopia (SCLH). Hum. Mol. Genet. 7, 1063–1070.
Di Filippo, M., Tozzi, A., Costa, C., Belcastro, V., Tantucci, M., Picconi, B., Calabresi, P., 2008. Plasticity and repair in the post-ischemic brain. Neuropharmacology 55, 353–362.
Doyle, K.P., Simon, R.P., Stenzel-Poore, M.P., 2008. Mechanisms of ischemic brain damage. Neuropharmacology 55, 310–318.
Elkabetz, Y., Panagiotakos, G., Al Shamy, G., Socci, N.D., Tabar, V., Studer, L., 2008. Human ES cell-derived neural rosettes reveal a functionally distinct early neural stem cell stage. Genes Dev. 22, 152–165.
Ferrara, A., El Bejaoui, S., Seyen, S., Tirelli, E., Plumier, J.C., 2009. The usefulness of operant conditioning procedures to assess long-lasting deficits following transient focal ischemia in mice. Behav. Brain Res. 205, 525–534.
Fujii, M., Hara, H., Meng, W., Vonsattel, J.P., Huang, Z., Moskowitz, M.A., 1997. Strain-related differences in susceptibility to transient forebrain ischemia in SV-129 and C57black/6 mice. Stroke 28, 1805–1810 (discussion 1811).
Gan, R., Lambert, C., Lianting, J., Chan, E.S., Venketasubramanian, N., Chen, C., Chan, B.P., Samama, M.M., Bousser, M.G., 2008. Danqi Piantan Jiaonang does not modify hemostasis, hematology, and biochemistry in normal subjects and stroke patients. Cerebrovasc. Dis. 25, 450–456.
Ginsberg, M.D., 2008. Neuroprotection for ischemic stroke: past, present and future. Neuropharmacology 55, 363–389.
Golanov, E.V., Reis, D.J., 1995. Contribution of cerebral edema to the neuronal salvage elicited by stimulation of cerebellar fastigial nucleus after occlusion of the middle cerebral artery in rat. J. Cereb. Blood Flow Metab. 15, 172–174.
Gorski, J.A., Zeiler, S.R., Tamowski, S., Jones, K.R., 2003. Brain-derived neurotrophic factor is required for the maintenance of cortical dendrites. J. Neurosci. 23, 6856–6865.
Gupta, S.K., Mishra, R., Kusum, S., Spedding, M., Meiri, K.F., Gressens, P., Mani, S., 2009. GAP-43 is essential for the neurotrophic effects of BDNF and positive AMPA receptor modulator S18986. Cell Death Differ. 16, 624–637.
Hartley, D.M., Kurth, M.C., Bjerkness, L., Weiss, J.H., Choi, D.W., 1993. Glutamate receptor-induced $^{45}Ca^{2+}$ accumulation in cortical cell culture correlates with subsequent neuronal degeneration. J. Neurosci. 13, 1993–2000.
Hastings, N.B., Gould, E., 1999. Rapid extension of axons into the CA3 region by adult-generated granule cells. J. Comp. Neurol. 413, 146–154.
Heurteaux, C., Laigle, C., Blondeau, N., Jarretou, G., Lazdunski, M., 2006a. Alpha-linolenic acid and riluzole treatment confer cerebral protection and improve survival after focal brain ischemia. Neuroscience 137, 241–251.
Heurteaux, C., Lucas, G., Guy, N., El Yacoubi, M., Thümmler, S., Peng, X., Noble, F., Blondeau, N., Widmann, C., Gobbi, G., Costentin, J., Debonnel, G., Lazdunski, M., 2006b. Deletion of TREK-1, a background potassium channel, results in a depression-resistant phenotype. Nat. Neurosci. 9, 1134–1141.
Huang, Z., Huang, P.L., Panahian, N., Dalkara, T., Fishman, M.C., Moskowitz, M.A., 1994. Effects of cerebral ischemia in mice deficient in neuronal nitric oxide synthase. Science 265, 1883–1885.
Illes, S., Theiss, S., Hartung, H.P., Siebler, M., Dihne, M., 2009. Niche-dependent development of functional neuronal networks from embryonic stem cell-derived neural populations. BMC Neurosci. 10, 93.
Jessell, T.M., Kandel, E.R., 1993. Synaptic transmission: a bidirectional and self-modifiable form of cell–cell communication. Cell 72 (Suppl.), 1–30.
Jin, K., Sun, Y., Xie, L., Peel, A., Mao, X.O., Batteur, S., Greenberg, D.A., 2003. Directed migration of neuronal precursors into the ischemic cerebral cortex and striatum. Mol. Cell. Neurosci. 24, 171–189.
Koh, J.Y., Choi, D.W., 1987. Quantitative determination of glutamate mediated cortical neuronal injury in cell culture by lactate dehydrogenase efflux assay. J. Neurosci. Methods 20, 83–90.
Lee, Y.S., Han, O.K., Park, C.W., Yang, C.H., Jeon, T.W., Yoo, W.K., Kim, S.H., Kim, H.J., 2005. Pro-inflammatory cytokine gene expression and nitric oxide regulation of aqueous extracted Astragali radix in RAW 264.7 macrophage cells. J. Ethnopharmacol. 100, 289–294.
Lesuisse, C., Martin, L.J., 2002. Long-term culture of mouse cortical neurons as a model for neuronal development, aging, and death. J. Neurobiol. 51, 9–23.
Lipsky, R.H., Marini, A.M., 2007. Brain-derived neurotrophic factor in neuronal survival and behavior-related plasticity. Ann. N. Y. Acad. Sci. 1122, 130–143.
Markakis, E.A., Gage, F.H., 1999. Adult-generated neurons in the dentate gyrus send axonal projections to field CA3 and are surrounded by synaptic vesicles. J. Comp. Neurol. 406, 449–460.
Martinez-Vila, E., Irimia, P., 2005. Challenges of neuroprotection and neurorestoration in ischemic stroke treatment. Cerebrovasc. Dis. 20 (Suppl. 2), 148–158.
Mattson, M.P., 2008. Glutamate and neurotrophic factors in neuronal plasticity and disease. Ann. N. Y. Acad. Sci. 1144, 97–112.
Meiri, K.F., Pfenninger, K.H., Willard, M.B., 1986. Growth-associated protein, GAP-43, a polypeptide that is induced when neurons extend axons, is a component of growth cones and corresponds to pp46, a major polypeptide of a subcellular fraction enriched in growth cones. Proc. Natl. Acad. Sci. U. S. A. 83, 3537–3541.
Nelles, G., Spiekermann, G., Jueptner, M., Leonhardt, G., Muller, S., Gerhard, H., Diener, H.C., 1999. Reorganization of sensory and motor systems in hemiplegic stroke patients. A positron emission tomography study. Stroke 30, 1510–1516.
Obrenovitch, T.P., Urenjak, J., Zilkha, E., Jay, T.M., 2000. Excitotoxicity in neurological disorders – the glutamate paradox. Int. J. Dev. Neurosci. 18, 281–287.
Oestreicher, A.B., De Graan, P.N., Gispen, W.H., Verhaagen, J., Schrama, L.H., 1997. B-50, the growth associated protein-43: modulation of cell morphology and communication in the nervous system. Prog. Neurobiol. 53, 627–686.
Pool, M., Thiemann, J., Bar-Or, A., Fournier, A.E., 2008. NeuriteTracer: a novel ImageJ plugin for automated quantification of neurite outgrowth. J. Neurosci. Methods 168, 134–139.
Rogers, D.C., Campbell, C.A., Stretton, J.L., Mackay, K.B., 1997. Correlation between motor impairment and infarct volume after permanent and transient middle cerebral artery occlusion in the rat. Stroke 28, 2060–2065 (discussion 2066).
Ryu, M., Kim, E.H., Chun, M., Kang, S., Shim, B., Yu, Y.B., Jeong, G., Lee, J.S., 2008. Astragali Radix elicits anti-inflammation via activation of MKP-1, concomitant with attenuation of p38 and Erk. J. Ethnopharmacol. 115, 184–193.
Schabitz, W.R., Sommer, C., Zoder, W., Kiessling, M., Schwaninger, M., Schwab, S., 2000. Intravenous brain-derived neurotrophic factor reduces infarct size and counterregulates Bax and Bcl-2 expression after temporary focal cerebral ischemia. Stroke 31, 2212–2217.
Sharp, F.R., Liu, J., Bernabeu, R., 2002. Neurogenesis following brain ischemia. Brain Res. Dev. Brain Res. 134, 23–30.
Siow, C.H., 2008. Neuroaid in stroke recovery. Eur. Neurol. 60, 264–266.
Strittmatter, S.M., Valenzuela, D., Kennedy, T.E., Neer, E.J., Fishman, M.C., 1990. G0 is a major growth cone protein subject to regulation by GAP-43. Nature 344, 836–841.
Sudhof, T.C., 1995. The synaptic vesicle cycle: a cascade of protein–protein interactions. Nature 375, 645–653.
Van Hooff, C.O., Holthuis, J.C., Oestreicher, A.B., Boonstra, J., De Graan, P.N., Gispen, W.H., 1989. Nerve growth factor-induced changes in the intracellular localization of the protein kinase C substrate B-50 in pheochromocytoma PC12 cells. J. Cell Biol. 108, 1115–1125.
Venketasubramanian, N., Chen, C.L., Gan, R.N., Chan, B.P., Chang, H.M., Tan, S.B., Picard, D., Navarro, J.C., Baroque 2nd, A.C., Poungvarin, N., Donnan, G.A., Bousser, M.G., 2009. A double-blind, placebo-controlled, randomized, multi-center study to investigate CHInese Medicine Neuroaid Efficacy on Stroke recovery (CHIMES Study). Int. J. Stroke 4, 54–60.
Volosin, M., Song, W., Almeida, R.D., Kaplan, D.R., Hempstead, B.L., Friedman, W.J., 2006. Interaction of survival and death signaling in basal forebrain neurons: roles of neurotrophins and proneurotrophins. J. Neurosci. 26, 7756–7766.
Wahlgren, N.G., Ahmed, N., 2004. Neuroprotection in cerebral ischaemia: facts and fancies–the need for new approaches. Cerebrovasc. Dis. 17 (Suppl. 1), 153–166.
Wang, L., Zhou, G.B., Liu, P., Song, J.H., Liang, Y., Yan, X.J., Xu, F., Wang, B.S., Mao, J.H., Shen, Z.X., Chen, S.J., Chen, Z., 2008. Dissection of mechanisms of Chinese medicinal formula Realgar–Indigo naturalis as an effective treatment for promyelocytic leukemia. Proc. Natl. Acad. Sci. U. S. A. 105, 4826–4831.
Zhang, S.C., Wernig, M., Duncan, I.D., Brustle, O., Thomson, J.A., 2001. In vitro differentiation of transplantable neural precursors from human embryonic stem cells. Nat. Biotechnol. 19, 1129–1133.
Zhang, R., Zhang, Z., Wang, L., Wang, Y., Gousev, A., Zhang, L., Ho, K.L., Morshead, C., Chopp, M., 2004. Activated neural stem cells contribute to stroke-induced neurogenesis and neuroblast migration toward the infarct boundary in adult rats. J. Cereb. Blood Flow Metab. 24, 441–448.
Zhang, R.L., Zhang, Z.G., Chopp, M., 2008. Ischemic stroke and neurogenesis in the subventricular zone. Neuropharmacology 55, 345–352.
Zhang, Y., Pardridge, W.M., 2001. Neuroprotection in transient focal brain ischemia after delayed intravenous administration of brain-derived neurotrophic factor conjugated to a blood–brain barrier drug targeting system. Stroke 32, 1378–1384.
Zuber, M.X., Goodman, D.W., Karns, L.R., Fishman, M.C., 1989. The neuronal growth-associated protein GAP-43 induces filopodia in non-neuronal cells. Science 244, 1193–1195.